

Quality Indices of Groundwater for Agricultural Use in the Soconusco, Chiapas, Mexico

Germán Santacruz de León^{1*}, José Alfredo Ramos Leal², Janete Moran Ramírez², Briseida López Álvarez¹, Eugenio Eliseo Santacruz de León³.

¹ Programa "Agua y Sociedad" de El Colegio de San Luis, A.C.

² Instituto Potosino de Investigación Científica y Tecnológica.

³ Universidad Autónoma Chapingo

ABSTRACT

In Soconusco, Chiapas, in spite of the high availability of surface water, it is resorting to the use of groundwater. Knowledge about the quality of surface or groundwater used to irrigate crops in that region is low. This paper aims to contribute to the knowledge of the quality of groundwater for agricultural use through the characterization of the spatial variability. Assuming a random spatial distribution of 45 samples which were collected in situ were determined: acidity and alkalinity (pH), electrical conductivity (EC), Total Dissolved Solids (TDS), cations and anions and trace elements; in addition to the agricultural index: Sodium Adsorption Ratio (SAR), Residual Sodium Carbonate (RSC), Soluble Sodium Percentage (SSP), Sodium Percentage (% Na), Kelly Ratio (KR), Magnesium Adsorption Ratio (MAR), Permeability Index (PI), Effective Salinity (ES), Salinity Potential (SP) and Osmotic Potential (OP). In general, SSP, % Na, KR, PI are low, there is only one anomalous point (9) with high values at W of the study area. Similarly, PS, ES, Cl, Na and SAR are low except point 16 and conversely, RSC and pH are high, except at this point located in the center of the study area. The results allow us to infer that the water in that aquifer presents no problems or sodicity toxic ions. In 27 sites sampled values above 250 $\mu\text{mhos/cm}$ were found at 25°C, classified as medium to high risk of salinity, unsuitable for agricultural use. Analysis of the combined effect of the presence of sodium (SAR) and salinity (EC or TDS) shows that 27 of analyzing sites have restricted water medium at very high for use in irrigation.

Keywords: Salinity; sodicity; osmotic pressure; sodium adsorption ratio; electrical conductivity; irrigation; acuífero.

Índices de calidad del agua subterránea para uso agrícola en el Soconusco, Chiapas, México

RESUMEN

En el Soconusco, Chiapas, a pesar de la alta disponibilidad de agua superficial, se recurre al uso del agua subterránea. El conocimiento de la calidad del agua superficial o subterránea utilizada para el riego de los cultivos en la región es bajo. Este trabajo contribuye al conocimiento de la calidad del agua subterránea para uso agrícola a través de la caracterización de su variabilidad espacial. Asumiendo una distribución espacial aleatoria, se colectaron 45 muestras, a las que se les determinó: acidez y alcalinidad (pH), conductividad eléctrica (CE), Sólidos Totales Disueltos (TDS), cationes y aniones y oligoelementos; además se determinaron índices agrícolas: Índice de adsorción de sodio (SAR), Carbonato de sodio residual (CSR), Porcentaje de sodio soluble (PSS), Porcentaje de sodio (% Na), Relación de Kelly (RK), Relación de Adsorción de Magnesio (RAM), Índice de Permeabilidad (IP), Salinidad Efectiva (SE), Salinidad Potencial (SP) y Potencial Osmótico (OP). En general, el PSS, %Na, RK, IP son bajas, sólo hay un punto anómalo (9) con valores altos en la parte oeste del área de estudio. Del mismo modo, SP, SE, Cl, Na y el RAS son bajas, excepto en el punto 16 y en contraste, CSR y pH son altos, excepto en este punto ubicado en el centro del área de estudio. Los resultados nos permiten inferir que el agua en ese acuífero no presenta problemas de sodicidad y de tóxicos. En 27 sitios se encontraron valores superiores a 250 $\mu\text{mhos/cm}$ a 25 ° C, clasificados como de riesgo medio a alto de salinidad, es decir inadecuados para uso agrícola. El análisis del efecto combinado de la presencia de sodio (RAS) y salinidad (CE o SDT) muestra que 27 de los sitios analizados presentan restricciones de medias a muy altas para su uso en riego.

Palabras clave: salinidad, sodicidad, presión osmótica, relación de adsorción de sodio, conductividad eléctrica, riego, acuífero.

Record

Manuscript received: 22/03/2017

Accepted for publication: 21/07/2017

How to cite item

Santacruz, G., Ramos, J. A., Moran, J., Lopez, B., & Santacruz, E. E. (2017). Quality Indices of Groundwater for Agricultural Use in the Soconusco, Chiapas, Mexico. Earth Sciences Research Journal, 21(3), 117 - 127.

doi:<http://dx.doi.org/10.15446/esrj.v21n3.63455>

Introduction

As the surface water, groundwater is part of the hydrological cycle and, a significant portion of the world population depends on it. Even there are zones of the world where, for climatic or geological reasons, is the only source (Price, 2003). In the past 50 years the groundwater has played a key role in agricultural production (Giordano and Villholth, 2007), currently, 50% of potable water and 45% of the irrigated agricultural area of the planet depend on groundwater (Rifat et al., 2014). In arid and semi-arid areas of Latin America, aquifers are the source of a third of the total water usage (Miletto et al. 2006).

In arid and semi-arid zones of Mexico, groundwater is the main source of supply. In the tropics unconfined aquifers are important sources of water for agriculture and domestic use. Six million hectares area irrigated, of which one third is irrigated with groundwater (Marín, 2002; Asad and Garduño 2004; CONAGUA, 2013).

Knowledge of groundwater quality in time and space, it is important to differentiate its composition and function of this, devoting it to best use. This would have generated different techniques for water quality report, include the so-called Water Quality Index (WQI) grouping one or more physicochemical and bacteriological parameters (Guzman-Colis et al. 2011; Kankal et al. 2012) even supported by statistical techniques (Hülya and Hayal, 2007; Papaioannou et al. 2010; Hafizan et al. 2011; Mohd et al. 2011). To this, the pressures of agriculture and increasing living standards demanding better agricultural products (Wijnen et al. 2012) and therefore better quality of water used for agricultural activity are added.

The quality of irrigation water has repercussions on the production; it may affect plant growth and thus reduce levels of agricultural production (Yesilnacar and Gulluoglu, 2008; Deshpande and Aher, 2012). To evaluate the quality of water for agricultural use, there are considered some aspects such as salinity, effects of sodium on soil properties and toxicity of specific ions (Ayers and Wescot, 1985) that are included in various guidelines for interpreting quality. These guidelines have been outfitted in various indices as the Sodium Adsorption Ratio (Richards, 1954), Magnesium Adsorption Ratio (Rifat, 2014) Soluble Sodium Percentage (Todd and Mays, 1980) Residual Sodium Carbonate (Eaton, 1950), among others (Table 1).

In Mexico the knowledge about the quality of groundwater for irrigation is scarce, it is considered as a requirement of lesser importance (Cardona et al., 2010). The Soconusco region in the state of Chiapas is in this condition (UNESCO, 2007 and 2010). There have been studies on the availability of water in the aquifer (Diaz, 2001; CONAGUA, 2009) and from them are considered relevant to study water quality in the Soconusco to reveal current conditions and that knowledge it can be referenced for farmers, agricultural planners and for future studies. The aim of this study was to analyze from the application of various indices, the spatial variation of the quality of groundwater for agricultural irrigation in the Soconusco region in the state of Chiapas, Mexico.

Materials and Methods

Localization and characterization of the study area

The aquifer of Soconusco is in the region of Soconusco, Chiapas. This area consists of sixteen municipalities, covering an area of 5,475.5 km² (Fig. 1). Agricultural activities are predominantly export-oriented crops such banana (*Musa paradisiaca*), mango (*Mangifera indica* L.), coffee (*Coffea* var.) and corn (*Zea mays*), soybean (*Glycine max*) and beans (*Phaseolus vulgaris*).

The climate is hot and humid type with temperatures ranging from 25-34 °C in spring and summer, while for the rest of the year temperatures are average values of 18-22 °C. It presents a rainfall ranging between 1,500 mm and 4,000 mm, with a regional average of 2,450 mm (JICA, 1999) due to the topographic variability. It is a region of great ecological diversity, with different strata termohídricos (Flottesmesch and Schriker, 1993) and the presence of different types of soils (Deinlein, 1993), which have their origin in volcanic ash.

HYDROGEOLOGICAL FRAMEWORK

The basis of the stratigraphic column that emerges in the Chiapas region is of Proterozoic age and is composed mainly of granitoids and orthogneises (Weber et al., 2006).

Covering discordant to the basal rocks, the rocks of the upper Paleozoic are represented by the detrital series belonging to the Paso Hondo and Grupera formations (López-Ramos, 1980), also by metamorphic rocks, including serpentinites, schists, gneisses and quartzites (Salas, 1975), which were intruded by granodiorites, diorites and granites, rocks of the Batolito of Chiapas.

Covering discordant to the sequence to the Paleozoic units are detrital-calcareous sediments (conglomerates, sandstones, limes and clays) that date from the Triassic and Jurassic, these are the Formations Todos Santos, Grupo Sierra Madre and Angostura (Morán-Zenteno, 1994).

Volcanic rocks cover all previous rocks and are composed of volcanic rocks whose composition ranges from acidic to basic from the Chiapaneco Volcanic Arc in the Cenozoic (Mora-Chaparro, et al., 2007).

Finally, the rocks of the Pliocene-Holocene are constituted by deposits of silts, sands, clays and pyroclastic deposits derived from the volcanic activities of the Chichonal and Tacaná; As well as by alluvial materials and residual soils.

The aquifer “Soconusco” is located in the physiographic province known as the Highlands of Chiapas, it is mainly distributed in the coastal plain, which is bounded on the south by the Pacific Ocean and west by the Sierra of Chiapas or the granite massif of Chiapas (Diaz, 2001; Macias et al., 2010).

Index	Equation	Reference
SAR	$\frac{Na^+}{\sqrt{\frac{Ca^{2+} + Mg^{2+}}{2}}}$	Richards, 1954
MAR	$\frac{Mg^{2+} \cdot 100}{Ca^{2+} + Mg^{2+}}$	Raghunath, 1987
PI	$\frac{(Na^+ + \sqrt{HCO_3^-}) \cdot 100}{Ca^{2+} + Mg^{2+} + Na^+}$	Doncen, 1964
%Na	$\frac{Na^+ + K^+}{Ca^{2+} + Mg^{2+} + Na^+ + K^+} \cdot 100$	Wilcox, 1955
SSP	$\frac{Na^+ \cdot 100}{Ca^{2+} + Mg^{2+} + Na^+}$	Todd and Mays, 1980
RSC	$(CO_3^{2-} + HCO_3^-) - (Ca^{2+} + Mg^{2+})$	Eaton, 1950
KR	$\frac{Na^+}{Ca^{2+} + Mg^{2+}}$	Kelly, 1963
ES	If $Ca > (CO_3^{2-} + HCO_3^- + SO_4^{2-})$, then $ES = \Sigma \text{ cations} \cdot -(CO_3^{2-} + HCO_3^-)$ If $Ca > (CO_3^{2-} + HCO_3^- + SO_4^{2-})$; but $Ca > (CO_3^{2-} + HCO_3^-)$, then $ES = \Sigma \text{ cations} \cdot -Ca^{2+}$ If $Ca > (CO_3^{2-} + HCO_3^-)$ but $(Ca^{2+} + Mg^{2+}) > (CO_3^{2-} + HCO_3^-)$, then $ES = \Sigma \text{ cations} \cdot -(CO_3^{2-} + HCO_3^-)$ If $(Ca^{2+} + Mg^{2+}) < (CO_3^{2-} + HCO_3^-)$, then $ES = \Sigma \text{ cations} \cdot -(Ca^{2+} + Mg^{2+})$	Palacios and Aceves, 1970
PS	$Cl^- + \frac{1}{2}SO_4^{2-}$	Palacios and Aceves, 1970
OP	$OP(atm) \approx CE(mS \cdot cm^{-1}) \times 0.36$	Wilcox, 1955
ESP	$\frac{100(-0.0126 + 0.01475 SAR)}{1 + (-0.0126 + 0.01475 SAR)}$	Richards, 1954

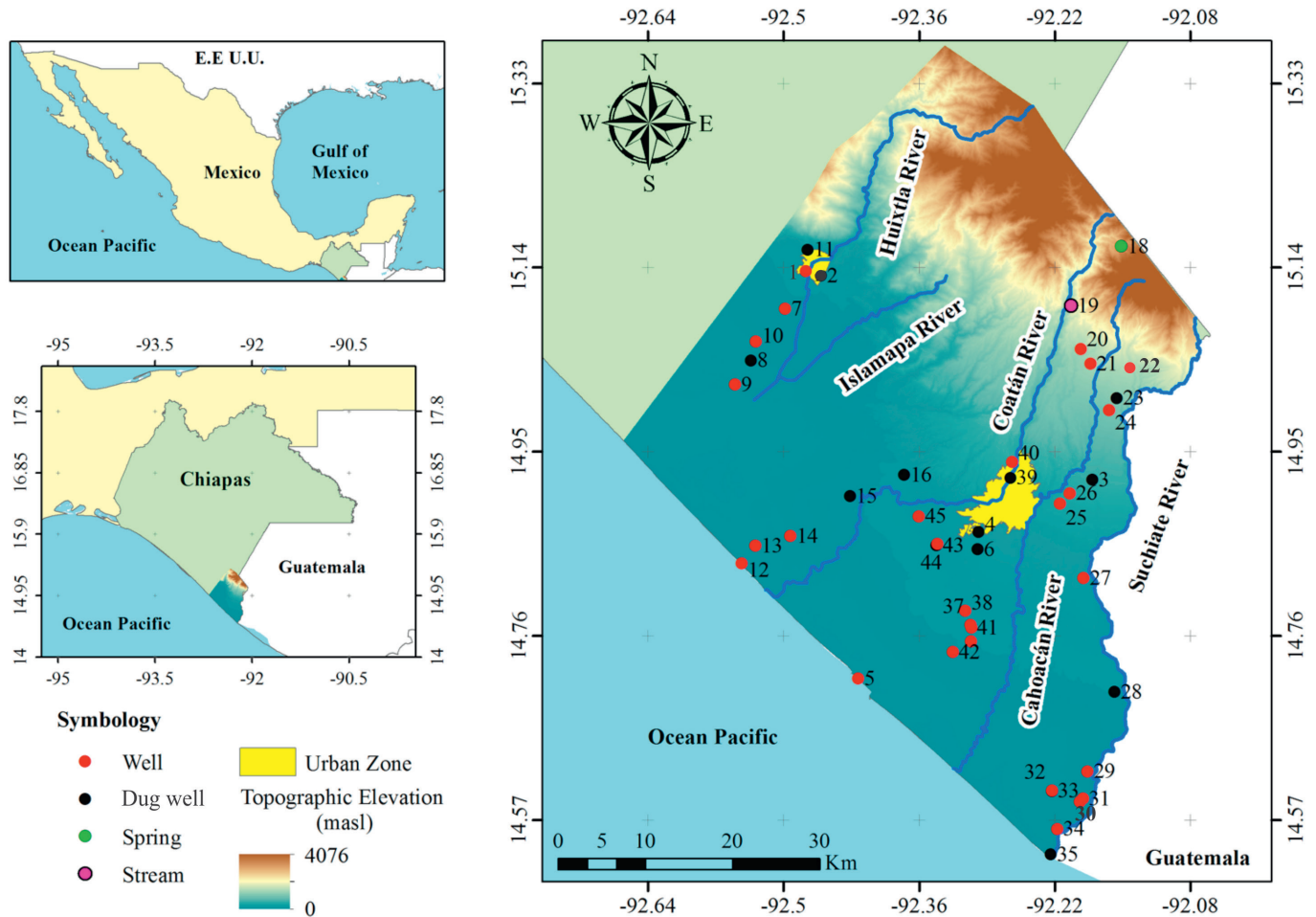


Figure 1. Location of the Soconusco aquifer and sampling points.

The granites and granodiorites are widely distributed in the Sierra of Chiapas, mainly in the northern part of the aquifer (recharge area). These rocks are one of the major sources for the formation of alluvial deposits and function as impermeable barriers to groundwater flow (Díaz, 2001; Macías et al., 2010). Volcanic rocks of basic and intermediate composition are composed of andesites and basalts, their permeability is relatively low, as it is compact enough rocks. However, the coastal plain has been formed by the accumulation of permeable sediments flowing down from the mountains in fluvial environments; and, by the processes of coastal marine type. This group of geological formations consists mainly of unconsolidated materials as clastic, sand, gravel, boulders and thin, such as clay and silt sediments, these sediments are those that constitute the aquifer (Díaz, 2001; Macías et al., 2010).

Hydrological balance

The hydrogeological balance of 2002 (CONAGUA, 2002) indicate that the volume of natural recharge is 885.9 million m³/year and 52.2 million m³/year of induced recharge, the actual evaporation is 325.4 million m³/year natural discharge (springs) is 442.2 mm³/year. The groundwater discharge to the sea is 27.7 million m³/year and extraction wells is 1.62 Mm³/year. With these figures, the CONAGUA (2002) considers the aquifer Soconusco in balance. In the 2009 update availability (CONAGUA, 2009) consider an average annual recharge of 938.2 Mm³/year. It is noteworthy that high rainfall in the region in combination with the presence of permeable materials in the plains allows high infiltration and soil washing.

Sampling and activities laboratory measurements

In February 2013 sampling was performed on 45 samples from springs, dug wells and wells, the samples were taken during the dry season to determine major cations and anions (Fig. 1). All samples were collected in bottles of high density polyethylene, washed and rinsed seven times with deionized water. The containers for collection of samples for the determination of cations and trace elements were washed with 10% hydrochloric acid. For each collected sample, was measured in situ, pH, EC, temperature, redox potential, dissolved oxygen, and alkalinity. Immediately after collection, the samples for cations and trace elements were acidified with pure nitric acid to pH <2. All samples were stored at a temperature below 4 °C. The major ions and trace elements were analyzed in the laboratory of the Centre for Geosciences, National Autonomous University of Mexico. Atomic Emission Spectroscopy was used with Inductively Coupled Plasma (ICP-OES) to determine the concentrations of cations higher calcium (Ca²⁺), magnesium (Mg²⁺), sodium (Na⁺) and potassium (K⁺) and higher sulphate anions (SO₄²⁻) and chloride (Cl⁻) were analyzed using liquid chromatography. Alkalinity and bicarbonate (HCO₃⁻) were determined by titration on the site. The ionic balance error (electro neutrality) in each of the 45 samples was considered less than 5%.

DRINKING WATER QUALITY ANALYSIS

To determine the quality of the groundwater for drinking purposes, WQI is computed according to the following relationship (Conesa, 1993):

Where C_i is percent value function assigned to the parameters, P_i weight assigned to each parameter and k constant taken from the values for the organoleptic characteristic (Table 2). k value in groundwater is normally 1, except in polluted water, which uses the values in Table 2.

Weight	Characteristic of water
1.0	For clear waters without apparent contamination
0.75	For waters with slight color, a scums and unnatural turbidity
0.50	For water with appearance of pollution and a strong odor
0.25	For dark waters that present fermentation and with a strong odor

CLASSIFICATION OF WATER IN CONNECTION WITH AGRICULTURAL USE

The classification of water for irrigation was made considering the conditions of acidity and alkalinity (pH), as well as sodicity rates as sodium adsorption ratio (SAR), the Residual Sodium Carbonate (RSC) is considered, the percentage Sodium Soluble (SSP), Sodium Percentage (% Na), the ratio Kelly (RK) and permeability index (PI) (Eaton, 1950; Todd and Mays, 1980). To evaluate and rank the water relative to saline conditions was considered to electrical conductivity (EC), Salinity Effective (SE), Salinity Potential (SP) and osmotic potential (OP) which is closely related to the EC and Total Dissolved Solids (TDS) (Palacios and Aceves, 1970; Aguilera and Martinez, 1996; Porta et al., 2010) the combination of these last three values allow classifying irrigation water. Likewise, the water is classified considering the combined effects of salinity and sodium contents employment diagram Salinity Laboratory of the Department of Agriculture of the United States and Wilcox Diagram. All indices were determined in a spreadsheet, by applying standard equations.

RESULTS AND DISCUSSION

The quality of data were analyzed based on their electroneutrality condition. The 45 groundwater samples perform that criterion.

In the study area, approximately 60% groundwater samples show distribution of mixed cations, 26 % are Na+K type, 8% are Ca and 6% are Mg Type water on Piper Trilinear Diagram. Among the major anions, 88% are plotted within the HCO₃ type, 6% are mixed type, 4% are SO₄ type and while only one sample has the influence of Cl type. The majority of the studied samples, are plotted in the Ca-HCO₃ type of water (60%), 18% are Na-Ca-HCO₃ type, 12% are Na-HCO₃ type, 6% are Ca-Mg-Cl type and 4% are Na-Cl type water on Piper Diagram (Fig. 2a).

The (Gibbs, 1970) diagram was originally constructed for surface water analysis; However, it is possible to recognize some processes that occur to groundwater. The three main mechanisms that control surface water chemistry can be defined as the domain of atmospheric precipitation (rainfall), rock dominance, and control of the evaporation-crystallization process (Gibbs, 1970). This diagram is constructed with the chemical data (anions and cations) of the groundwater samples.

The graph of TDS vs. Na/(Ca + Na) of The Gibbs diagram (1970) indicates the dominance of dilution by mixing, rock alteration in the study area and in another group the evaporation process predominates (Fig. 2b).

The quality of water for human consumption indicates that 64% of the analyzed samples have very good quality, 20% have medium quality and 7% have poor or excellent quality and only 2% have very poor quality (Fig. 2c).

Terms of acidity and alkalinity

The quality of water used for irrigation significantly influences the productivity of crops, depending on the presence of dissolved salts in it and their concentrations. Salts change the osmotic processes, and the presence of toxic substances (such as boron) can affect the metabolic processes in plants. The maximum and minimum pH values are 9.2 (point 19) and 6.1 (point 21), respectively. Three (points 18, 19 and 36) of the 45 samples, have pH values above 8.5 and all are above 6 (Fig. 3a).

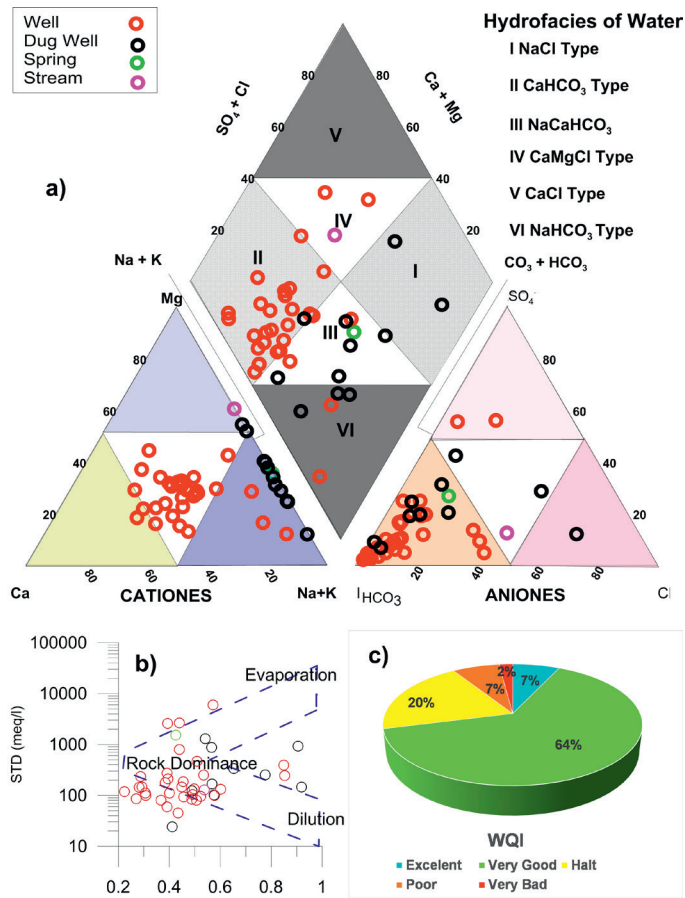


Figure 2. a) Piper diagram of the groundwaters of the study area, b) Gibbs diagram showing the mechanisms controlling the chemistry of groundwater of major cations c) Graph showing the distribution of the water quality of Soconusco aquifer.

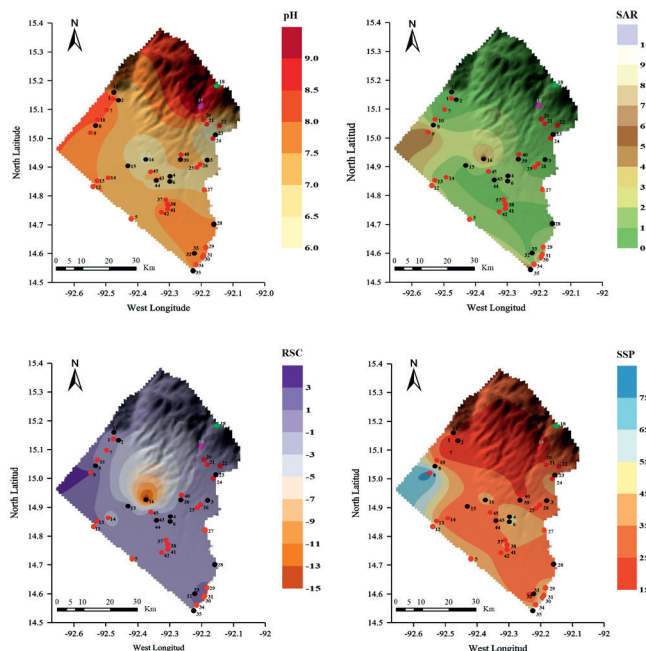


Figure 3. Spatial Distribution of Indices a) pH, b) Sodium Adsorption Ratio (SAR), c) Residual Sodium Carbonate (RSC) and d) Soluble Sodium Percentage (SSP).

Values above pH 8.5 and below 6 are indicative of an abnormal water quality are a signal of the presence of an ion toxic to crops. Water with pH values within this range creates conditions of assimilation of different nutrients such as phosphorus and some micronutrients (Ayers and Wescot, 1985).

Terms of sodicity

The presence of sodium in water at concentrations considerable permeability can affect the rate of infiltration and soil tillage (Romero, 2009), so that a high proportion of sodium relative to the calcium concentration causes a decrease in infiltration its dispersing effect on soil aggregates (Grattan and Oster, 2003 Ruda 2005). The data for assessing the quality of water relative to sodium are the SAR, the RSC, the SSP, the % Na, the RK and the PI. There is more possibility of sodification if the proportion of sodium is high with respect to the presence of calcium and magnesium (Peinado-Guevara et al., 2011).

The maximum and minimum values are 10.77 SAR (point 35) and 0.27 (point 22) respectively (Fig. 3b). This index shows that there is no danger of sodicity in water drawn from the aquifer Soconusco, only use No. 35 presents values above 10, which is the lower limit for classifying water as well. (Fig. 3b).

The presence of carbonates and bicarbonates have effects on the quality of water for irrigation, when their presence is greater than the concentration of calcium plus magnesium exists the possibility of forming carbonates of sodium, causing deflocculation soil (Palacios and Aceves, 1970; Aguilera and Martinez, 1996), the agricultural land irrigated with such water may become infertile (Rifat et al., 2014). The RSC indicates the danger of sodium carbonate, when the cations have already reacted with carbonates and bicarbonates of calcium and magnesium, to predict the trend of these cations to precipitate in the soil when irrigated with highly carbonated water (Peinado-Guevara et al., 2011). Four samples (items 9, 13, 29, 30) have RSC values, higher than 1.25 meq/L (Fig. 3c), the rest shows values below this limit and are considered safe for use in agricultural irrigation. The maximum and minimum values, are 3.55 RSC (point 30) and -15.38 (point 16), respectively.

Displacement of calcium and magnesium in the cation exchange process initiated when the sodium content in solution is greater than 50% of the cations (Palacios and Aceves, 1970, Aguilera and Martinez, 1996), high percentages of sodium in water (greater than 50%) used in irrigation, prevents the growth of crops and reduce soil permeability (Rifat et al., 2014), SSP values below 50 indicate good water quality and above this value indicate that the water is not suitable for irrigation (Fig. 3d). The maximum value found in this sample was 80.02 (item 9) and the minimum was 15.2 (point 33), four harvesting (items 9, 12, 30, 35) present above the limit of 50 values (Fig. 3d).

Groundwater can be grouped according to their sodium content in percent (% Na), these are considered excellent for use in agricultural irrigation, and have lower values when 20%, good values 20-40%, with permissible values 40-60%, 60-80% doubtful and unsuitable when presenting values above 80% (Wilcox, 1955). The maximum and minimum values found in the aquifer under study are 80.8% and 18.4%. Three points (2, 7 and 33) have classified as excellent water; 24 exploitations have classified as good quality water; 14 have classified as admissible water; two points present a classification of water considered doubtful and as suitable for use in agriculture (Fig. 4a).

The presence of sodium with respect to the calcium plus magnesium concentration is measured by the rate or the Kelly index, values greater than 1 indicate excess sodium in water, and values less than 1 indicate that water is suitable for use in agricultural irrigation (Aher and Deshpande, 2011; Deshpande and Aher, 2011, 2012). The maximum and minimum values for the aquifer Soconusco were 4.01 and 0.18, respectively; four points (9, 12, 30 and 35) have values greater than 1 (Fig. 4b).

Soil permeability is affected by the presence of sodium, calcium, magnesium, and bicarbonate in irrigation water when it is applied continually. Considering this index water is classified as Class I and Class II if it has more than or equal to 75% PI, this water is considered good quality for use in irrigation. In Class III, the water presents values lower than PI 25% (Joshi et al., 2009;

Ishaku et al. 2011; Obiefuna and Sheriff, 2011). In this study the maximum and minimum values of PI were 161.5% and 46.5% (Fig. 4c), respectively, so we can conclude that the Soconusco aquifer is of good quality for irrigation.

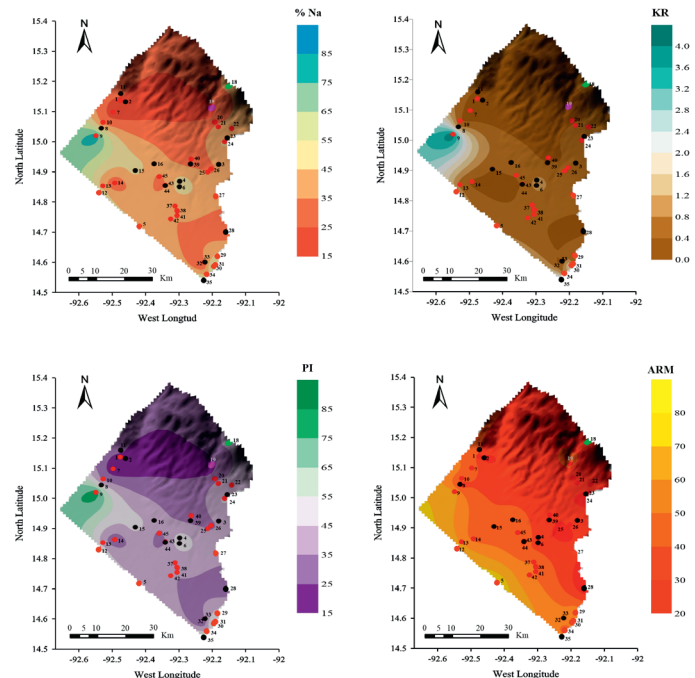


Figure 4. Spatial distribution of the indices a) % Na, b) Kelly ratio (KR), c) Permeability indices (PI) and d) Magnesium Adsorption Ratio (MAR).

In most of the water, calcium and magnesium remain in equilibrium, the presence of magnesium in concentrations affecting agricultural production sensitive to the chemical component (Nagaraju et al., 2006) cultures. In general groundwater containing low concentrations of magnesium can be higher if the water is in contact with dolomite containing high concentrations of it, its content in the water is a relevant indicator for the classification of water for use in irrigation. The index allows to evaluate Magnesium Adsorption Ratio (MAR), that provides percentage values greater than 50%, causes harmful effects on soil (Obiefuna and Sheriff, 2011; Nag and Ghosh, 2013; Rifat et al., 2014) values. The maximum and minimum values found in this study were 79.5% (point 5) and 20.2% (point 29), respectively. Only 10 of the 45 sites sampled 50% have higher values, which are located very close to the coastline (Fig. 4d).

Salt conditions

High concentrations of salts in irrigation water can cause an increased presence of salts in the root zone and accumulation in the soil profile, causing reduction in growth, development and production of agricultural crops (Grattan and Oster, 2003; Romero 2009). The presence of salts affects the OP and reduces crop yields (Palacios and Aceves, 1970; Aguilera and Martinez, 1996). EC measures the presence of salts in the water; it is directly proportional to the concentration of salts in solution (Palacios and Aceves 1970; Aguilera and Martinez, 1996; Porta et al., 2010). Other criteria to evaluate the conditions of salinity in the water are the SE and SP (Aguilera and Martinez 1996; Porta et al., 2010) and the OP that is closely related to the EC and with the TDS, the conjunction of the latter three values allows to classify irrigation water (Palacios and Aceves, 1970, Aguilera and Martinez, 1996, Porta et al., 2010).

Salinity is considered the most important criterion for classifying irrigation water (Ghasseme et al., 1995), salinity in soils causes reduced productivity (Essien and ubit, 2013). Electrical conductivity is a measure of the risk of salinity, the excess of it reduces the osmotic activity and interferes with the uptake of water and nutrients from the soil to the plant, so while the higher the EC less water will be available to plants (Nagaraju et al. 2006; Joshi

et al. 2009, Ishaku et al., 2011, Obiefuna and Sheriff, 2011; Nag and Ghosh, 2013). EC values under 250 $\mu\text{mhos/cm}$ at 25 °C in the irrigation water are considered excellent (C1) of 250-750 are classified as good (C2) of 750-2000 (C3) are admissible in 2000-3000 (C4) is considered to be doubtful use, so the water above 3000 $\mu\text{mhos/cm}$ at 25 °C values (C5) are considered inadequate, since soil salinity tends to increase in proportion to the concentration of salts in the water that is irrigated (Hamdy et al., 1993, Sharma and Rao 1998; Perez-Sirvent et al., 2003), the concentration of salts in the soil can be two to six times corresponding to conductivity of irrigation water (Hamdy et al., 1993; Perez-Sirvent et al., 2003).

In this study, the maximum and minimum values of CE (Fig. 5a) were 3995 $\mu\text{mhos/cm}$ at 25 °C and 49 $\mu\text{mhos/cm}$ at 25 °C. 19 of 45 sampling points have lower values than 250 $\mu\text{mhos/cm}$ at 25 °C, 18 points have values between 250-750, three point has classified as admissible water; the rest of the sampling points, 5 of 45 had higher values at 2000 $\mu\text{mhos/cm}$ at 25 °C, ie, they are unsuitable for use in agriculture (Fig. 5a) waters. In an area

near the aquifer under study Olea (2013) found values ranging from 152 EC $\mu\text{mhos/cm}$, in wells near the city of Huixtla, to 31,700 values $\mu\text{mhos/cm}$ wells or very close to the shoreline wells.

EC values found in the Soconusco aquifer, suggest that are mild problems of salinity, although the SE and SP indicate that the water from this aquifer is generally of good quality. Considering the above, it was deemed appropriate to classify the water according to OP and the presence of TDS. OP values below 0.1 atm are indicators of some saline water with excellent quality, values between 0.1-0.3 are indicators of saline water with good quality, values of 0.3-0.7 indicates saline water with allowable quality water, point between 0.7-1.1 very saline water with growing problems and values greater than 1.10 atm OP indicators are very saline water with significant problems. The results of this index for the Soconusco aquifer show that 4 points has excellent water quality, 26 points have saline water of good quality; 9 are classified allowable salt water quality and other points (6 of 45) are classified as very saline water with major problems.

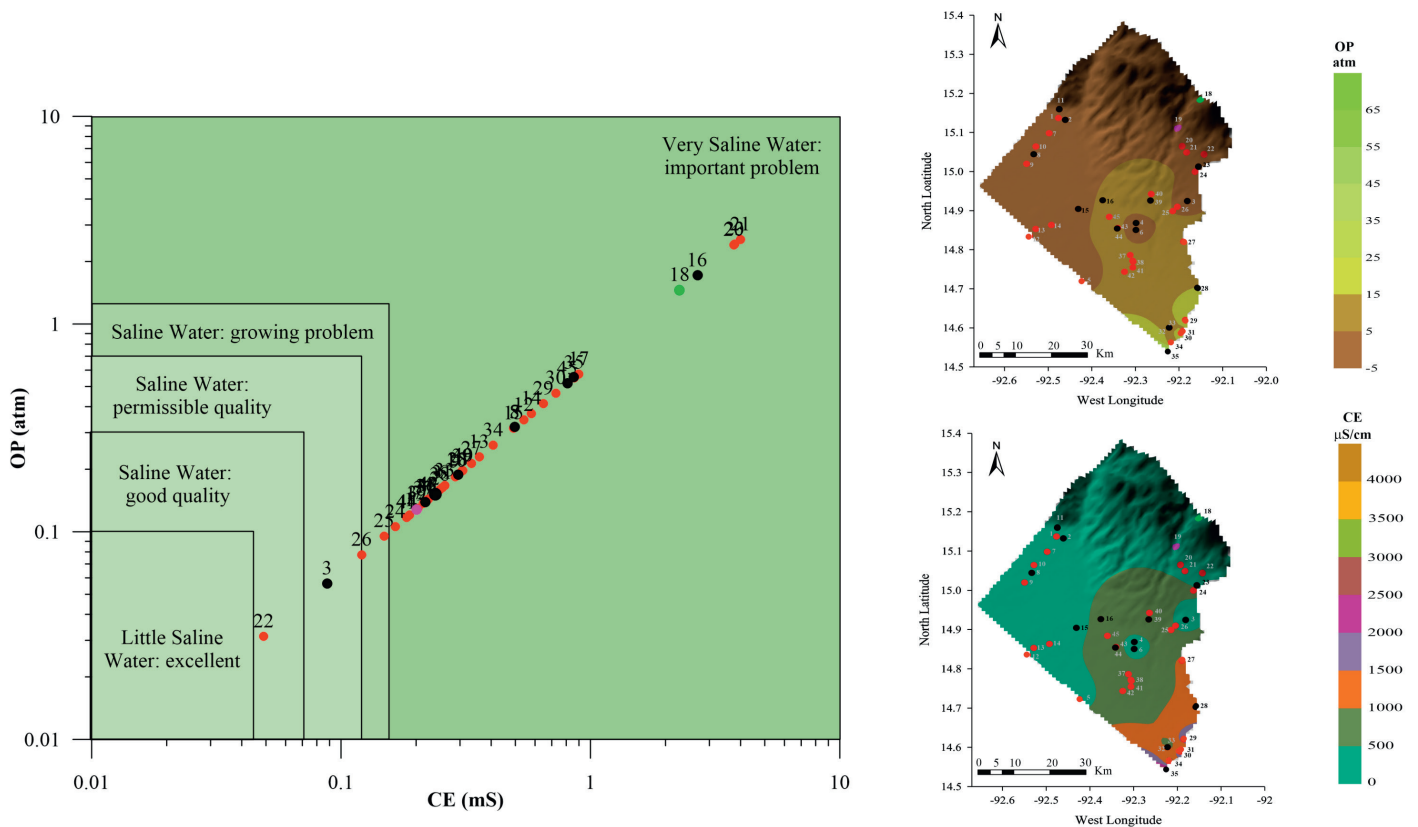


Figure 5. Spatial distribution of the indices a) Osmotic Potential (OP) vs Electrical Conductivity (EC), b) Osmotic potential (OP) and c) Electrical conductivity (EC).

Concerning TDS, if these values are between 0-1000 mg/L it is considered non-salt fresh water if they are between 1000-3000 mg/L slightly saline, of 3000-10000 is considered moderately saline, values TDS above 10000 mg/L are indicative of highly saline waters. The minimum and maximum values of TDS for this study are 87 mg/L and 50,760 mg/L. About the 45 samples taken from the Soconusco aquifer, 40 are classified as non-salt fresh water, 4 are classified as slightly saline, 1 is classified as moderately saline. It is important to remember that the presence of dissolved water in excessive amounts ions cause physical and chemical effects on the soil and plants (Ahamed et al., 2013), reduces the ability of plant roots to extract water from the ground. There is a direct relationship between the presence of salts, measured from the EC, and the OP. Thus, as noted above, most of the

samples water from wells in the Soconusco aquifer are between non-salt fresh water to considered non-salt fresh water (Fig. 5c).

The more realistically estimated danger of salinization, since it considers that the soluble salts of irrigation water are incorporated to soil, taking into account the precipitation of less soluble salts such as calcium and magnesium carbonates; as well as calcium sulphate (Rodriguez et al., 2008, Mancilla, 2012, Barrios, 2014). Similarly, the SP to estimate the risk that can generate the salts when the moisture content in soil is low, it is considered as one of the best estimates of the effect of salts on plants (Rodriguez et al., 2008), considers the precipitation of less soluble salts such as chlorides and sulfates (Nagaraju et al., 2006; Mancilla, 2012; Barrios, 2014), leading to increases in osmotic pressure and reduced crop production.

The maximum and minimum values of ES obtained in this study were 30.04 meq/L (point 16) and 0.15 meq/L (point 20), respectively. Of the 45 water samples taken in the Soconusco aquifer, 37 ES presented values lower than 3, which is the upper limit for classification as good quality water. Six exploitation (items 9, 12, 14, 17, 29 and 30) have water classified as conditional (with ES values above 3 but less than 15) and two harvests (points 16 and 35) are classified as not recommended water ES with values greater than 15. With respect to the PS results indicate that the maximum value was 27.9 (Item 16) and the minimum was 0.06 (point 34), the same limits used in the ES are applied to classify water in respect to the PS; according to the above 42 of the 45 samples fall in the classification of good quality water; two (points 14 and 35) have conditioned water and one (point 16) is classified as not recommended (Figs. 6a, 6b and 6c).

Classification water considering the % Na, the SAR and the EC

The combination of SAR and EC values for each of the sampling points were plotted in the diagram developed by the Laboratory of the US Salinity (Fig. 7a), the chart allows classification of irrigation water. About the 45 samples collected in the in Soconusco aquifer, 19 points are classified as C1S1 water, ie, low risk of salinity and low risk of sodification. Eighteen of the 45 samples are classified as C2S1 (medium risk and low risk of salinity sodification). Two samples (points 17 and 45) fall into the classification C3S1 and which are at high risk of salinity and low risk of sodification. Four samples (points 18, 20, 21 and 23) are classified as C4S1, which should be only used on soils with good water permeability. The use of water from the Soconusco aquifer is conditioned by the salinity levels rather than those of sodification. But also points 16 and 35 begin to show signs of high and very high risk of sodification.

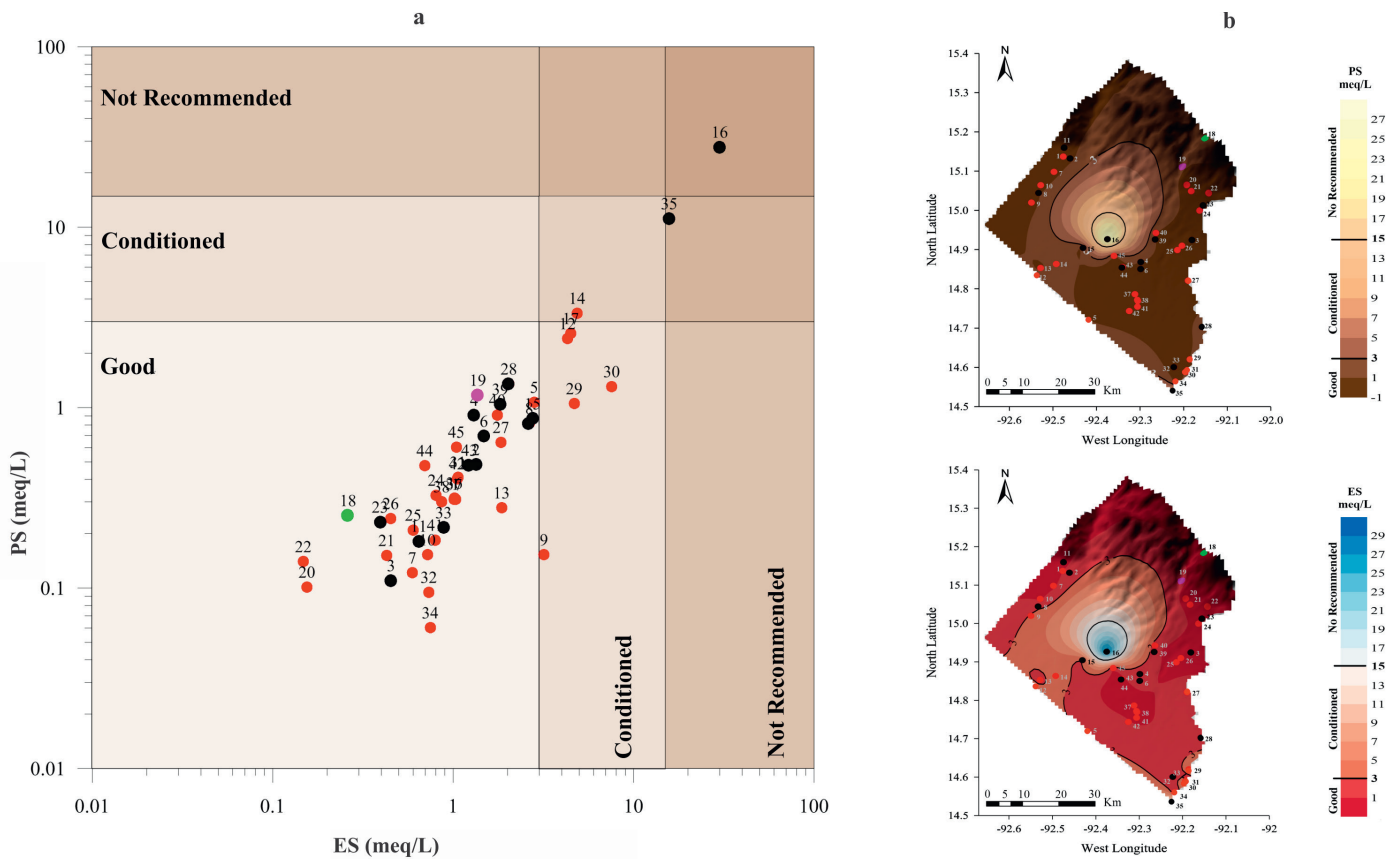


Figure 6. Spatial distribution of the indices a) Effective salinity (ES) vs potential salinity (PS), b) Potential salinity (PS) and c) Effective salinity (ES).

The % Na is plotted together with the EC in the diagram Wilcox and it classifies water for use in irrigation (Fig. 7b). 36 of the samples collected fall into the classification of good to excellent, 2 are considered permissible to good, both fall into the category of admissible doubtful

equal number of samples (points 18 and 16) are classified as doubtful inadequate, notably, 3 of the 45 samples taken from the Soconusco aquifer are classified as inadequate (Fig. 7b). It is worth remembering that there is no precedent studies on water quality to serve as reference.

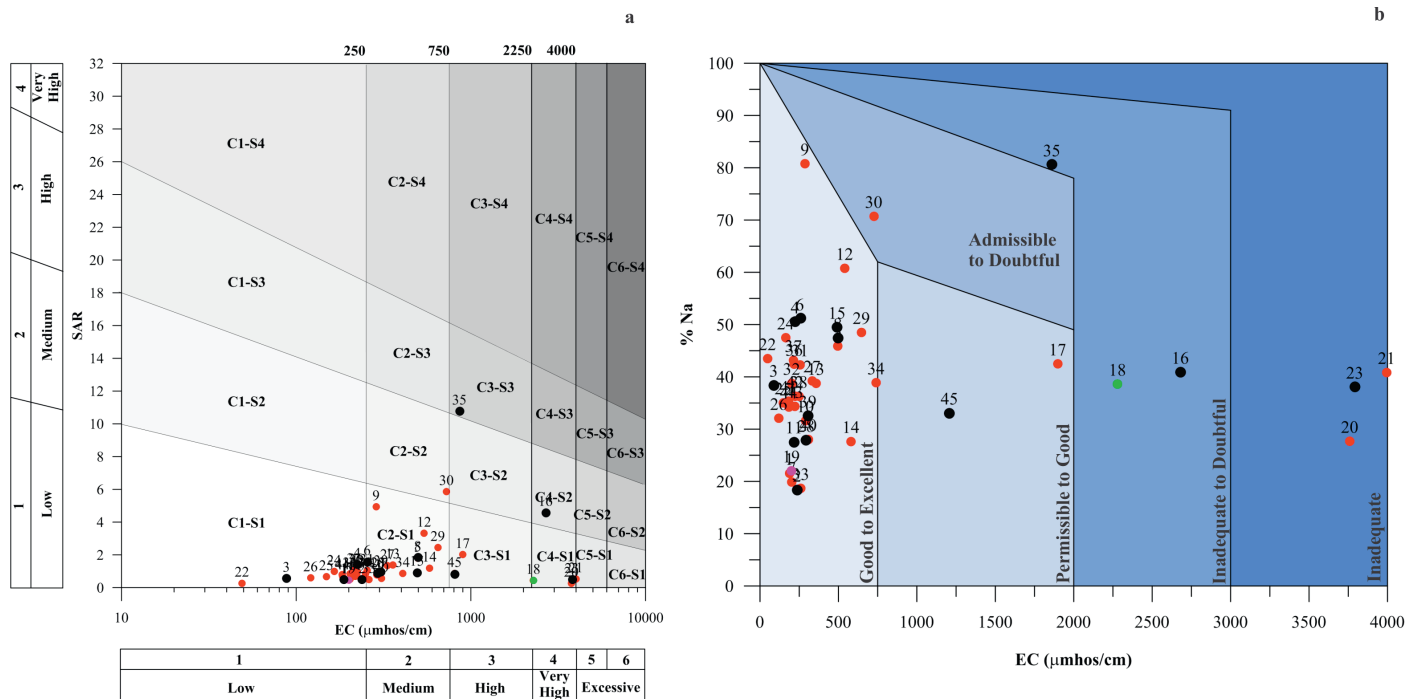


Figure 7. Water classification according to a) Wilcox y) Electrical Conductivity (EC) vs Percent Sodium (% Na), for the Soconusco aquifer.

The previous analysis pointed out that the problems associated with the aquifer sodicity Soconusco are not considered and are presented in specific areas; However, the problems associated with salinity may increase, although they have not seen yet and there are no studies that indicate problems of soil salinization in the study region, which is due in great measure to the heavy rainfall, the soil conditions, climate and, above all, hydrogeochemical Soconusco.

Presence of toxic ions (chloride and sodium) for plants

Some ions, depending on the concentration in which they are in the water, can be toxic to crops, usually they accumulate in leaves. Often toxic chlorine ions, sodium and boron (Ayers and Wescot 1985. If the chloride concentration exceeds crop tolerance may result from the burning of leaves to tissue death, when the content of this element is less than 4 meq/L, the water is classified as good, if it is between 4-10 meq/L is classified as conditional, and if you have concentrations above 10 meq/L are classified as not recommended water. The maximum value found in this study was 21.5 meq/L (point 16) and the minimum was 0.03 meq/L, with a coefficient of variation of 11.22. Of the 45 samples, 43 presented below 4 meq/L (Fig. 8a) values, indicating that the Soconusco aquifer presents no problems according to this chemical element and is classified as good ie may be used for irrigation.

Sodium often causes similar damage causing chlorides and nutritional imbalances in plants. Values less than 3 meq/L of Na are indicative of low toxicity hazard to plants of this; values 3-9 meq/L indicate medium risk and values of more than 9 meq/L are high risk indicators for sodium. The maximum and minimum values obtained in this sample were 16.6 meq/L and 0.07 meq/L, respectively, with a coefficient of variation of 5.6. In 38 of the 45 samples collected, sodium values obtained are less than 3 meq/L, ie it is endangered by water with low sodium. Five samples (points 9, 12, 17, 29 and 30) have values between 3 and 9 meq/L, indicating water at average risk. Two samples (points 16 and 35) have more than 9 meq/L values at high risk for sodium (Fig. 8b).

CONCLUSIONS

- Geochemistry of groundwater of Soconusco display the order of ionic abundance is $\text{Na}^+ > \text{Ca}^{2+} > \text{Mg}^{2+} > \text{K}^+$ and $\text{HCO}_3^- > \text{SO}_4^{2-} > \text{Cl}^-$ trend.
- The type of water that predominate in the study area is Ca-HCO_3 type.
- The main hydrochemical processes occurring in groundwater are dilution by mixing, water-rock interaction and only some samples show evaporation effects.
- WQI indicate that more than half samples are not suitable for drinking purposes (60% is very good quality).
- The groundwater of the Soconusco aquifer has no problems of sodicity for agricultural use.
- The soil, climatic and physiographic conditions, as well as rainfall of around 1,500 to 4,000 mm/year in the region, favor the recharge of the aquifer and the adequate mechanisms for the natural drainage of the aquifer, avoiding the salinity of groundwater.
- The combination of PS/ES, classifies most of the water as good for agricultural use, only some samples fall as conditioned and two samples as not recommended for this use.
- The combination of % Na/EC, classifies the groundwater of the Soconusco aquifer, as excellent, only some as admissible to doubtful and very few are classified as doubtful to inadequate.

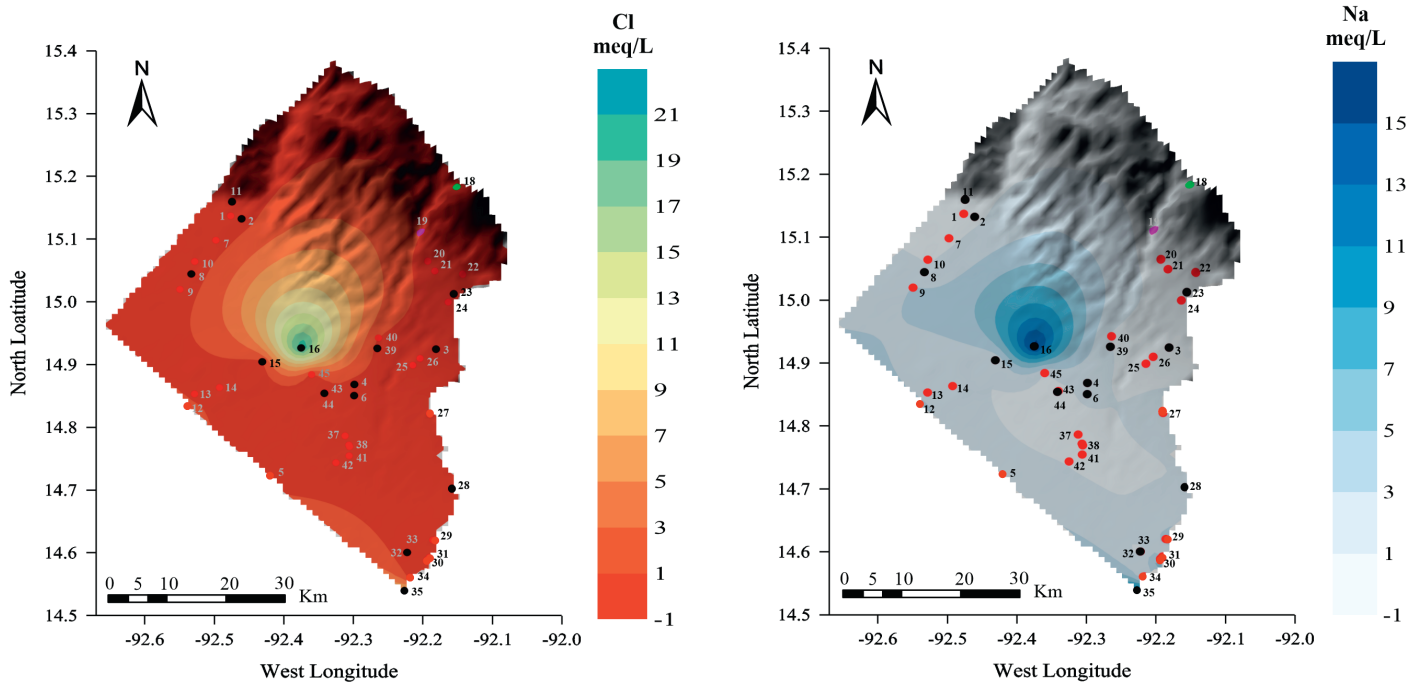


Figure 8. Spatial distribution of toxic ions a) ion Cl and b) Na, for the Soconusco aquifer.

REFERENCES

- Aguilera, M. & Martínez, R. (1996). *Relaciones agua suelo planta atmósfera*. 4a ed. Departamento de Irrigación. México: Universidad Autónoma Chapingo.
- Ahamed, J., Loganathan, K. & Ananthkrishnan, S. (2013). A comparative evaluation of groundwater suitability for drinking and irrigation purposes in Pugalur area, Karur district, Tamilnadu, India. *Archives of Applied Science Research*, 5(1), 213-223. Retrieved from: <http://scholarsresearchlibrary.com/aasr-vol5-iss1/AASR-2013-5-1-213-223.pdf>
- Aher, K.R. & Deshpande, S.M. (2011). Assessment of water quality of the Maniyad Reservoir of Parala Village, district Aurangabad: Suitability for multipurpose usage. *International Journal of Recent Trends in Science and Technology*, 1(3), 91-95. Retrieved from <https://www.statperson.com/Journal/ScienceAndTechnology/Article/Issue3/Assessment.pdf>
- Asad, M. & Garduño, H. (2004). Documento de trabajo-34636. *Gestión de Recursos Hídricos en México: El papel del PADUA en la sostenibilidad hídrica y el desarrollo rural*. México. Banco Mundial: Retrieved from: <http://documentos.bancomundial.org/curated/es/2004/06/6966415/water-resources-management-mexico-role-water-rights-adjustment-program-wrap-water-sustainability-rural-development-gestion-de-recursos-hidricos-en-mexico-el-papel-del-padua-en-la-sostenibilidad-hidrica-y-el-desarrollo-rural>
- Ayers, S. & Westcot, D. (1985). *Water Quality for Agriculture*. Rome. *FAO irrigation and drainage paper 29*. Rome, Italy: Food and Agriculture Organization of the United Nations.
- Barrios Castillo, I. (2014). *Calidad de aguas naturales y residuales en el sistema hidrográfico del Valle del Mezquital, Hidalgo, México*. (Tesis de maestría). Colegio de Posgraduados, Montecillo, México.
- Cardona, A. & Carrillo-Rivera, J.J., Herrera-Zamarrón, G. & López-Álvarez, B. (2010). La contaminación del agua subterránea en México. En Aguilera, A. (Coord.), *Calidad del agua: un enfoque multidisciplinario* (pp. 55-77), México D.F.: Universidad Nacional Autónoma de México. Instituto de Investigaciones Económicas.
- CONAGUA (2002). *Determinación de la disponibilidad de agua en el acuífero Soconusco, Estado de Chiapas*. Subgerencia de Evaluación y Modelación Hidrogeológica. Gerencia de Aguas Subterráneas. Subdirección General Técnica. Comisión Nacional del Agua. México. [en línea]. Retrieved from: <http://207.248.177.30/mir/uploadtests/1827.66.59.7.2B-2-SOCONUSCO%20FINAL%20cuadernillo%20MIR-1.doc> 25/07/2014
- CONAGUA (2009). *Actualización de la disponibilidad media anual de agua acuífero (=/=) Soconusco, Estado de Chiapas*. Subdirección General Técnica. Gerencia de Aguas Subterráneas. Subgerencia de Evaluación y Ordenamiento de Acuíferos. Comisión Nacional del Agua. México.
- CONAGUA (2013). *Estadísticas del Agua en México*, Edición 2013. Secretaría de Medio Ambiente y Recursos Naturales. Comisión Nacional del Agua. México.
- Fernández-Vitoria, C.F. (1993). *Guía Metodológica para la Evaluación del Impacto Ambiental*. Madrid: Ediciones Mundi-Prensa.
- Deinlein, R. (1993). Algunos ejemplos del desarrollo de los suelos en diferentes niveles altitudinales en el Soconusco. En Richter, M (Ed.), *Investigaciones Ecogeográficas sobre la Región del Soconusco, Chiapas* (pp. 35-48). Chiapas, México: Centro de Investigaciones Ecológicas del Sureste.
- Deshpande, S.M. & Aher, K.R. (2011). Quality Characterization of Groundwater from Tribakeswar-Peth area of Nashik District and its suitability for domestic and irrigation purpose. *Gondwana Geological Magazine*, 26(2), 157-162.
- Deshpande S.M. & Aher K.R. (2012). Evaluation of Groundwater Quality and its Suitability for Drinking and Agriculture use in Parts of

- Vaijapur, District Aurangabad, MS, India. Resarch Journal of Chemical Sciences, 2(1), 25-31. Retrieved from http://isca.in/rjcs/Archives/vol2/i1/04.ISCA-RJCS-2011-216_Done.pdf
- Díaz, J. (2001). *Simulación numérica del flujo subterráneo en el acuífero del Soconusco, Chiapas*. (Tesis de Maestría.) Facultad de Ingeniería. División de Estudios de Posgrado. Universidad Autónoma de México. México.
- Eaton F.M. (1950). Significance of carbonates in irrigation water. *Soil Science*, 69(2), 123-133.
- Essien O. E. & Ubit, F. (2013). Investigation of Ikpa river water quality with consideration for domestic and agricultural uses. *Wudpecker Journal of Agricultural Research*, 2(11), 315-323. Retrieved from <http://www.wudpeckerresearchjournals.org/WJAR/pdf/2013/November/Essien%20and%20Ubit.pdf>
- Flottemesch, F. & R. Schriker (1993). Investigación sobre la micro y mesoclimatología en la región del Soconusco. En Richter, M. (Ed.), *Investigaciones Ecogeográficas sobre la Región del Soconusco, Chiapas* (pp. 94-115). Chiapas, México: Centro de Investigaciones Ecológicas del Sureste.
- Ghassemi, F., Jakeman, A.J., & Nix H.A. (1995). *Salinization of land and water resources. Human causes, extent, management and case studies*. United Kindom, Centre for Resource and Environmental Studies. Australian National University: CABI.
- Gibbs, R.J. (1970). Mechanisms controlling world water chemistry. *Science*, 170(3962), 1088-1090. Doi: 10.1126/science.170.3962.1088
- Giordano, M. & Villholt K.G. (Eds.). (2007). *The agricultural groundwater revolution. Opportunities and threats to development*. Colombo, Sri Lanka: International Water Management Institute.
- Grattan, S. R. & Oster, J. D. (2003). Use and Reuse of Saline-Sodic Waters for Irrigation of Crops, *Journal of Crop Production*, 7(1-2), 131-162.
- Guzmán-Colis, G., Thalasso, F., Ramírez-López, M., Rodríguez-Narciso, E., Guerrero-Barrera, A. & Avelar-González, F. (2011). Evaluación espacio-temporal de la calidad del agua del río San Pedro en el estado de Aguascalientes, México. *Revista Internacional de Contaminación Ambiental*. 27(2), 89-102. Recuperado de <http://www.journals.unam.mx/index.php/rica/article/viewFile/25007/23588>
- Hafizan, J., Sharifuddin, M., Mohd, K., Tengku, H., Mohd, A., Mohd, E. & Mazlin, M. (2011). Spatial water quality assessment of Langat River Basin (Malaysia) using environmetric techniques. *Environmental Monitoring Assessment*, 173(1-4), 625-641. DOI 10.1007/s10661-010-1411-x
- Hamdy, A., Abdel-Dayem, S. & Abu-Zeid, M. (1993). Saline water management for optimum crop production. *Agricultural Water Management*, 24(3), 189-203.
- Hülya, B. & Hayal, B. (2007). Surface Water Quality Assessment by Environmetric Methods. *Environmental Monitoring Assessment*, 131(1-3), 371-376. DOI:10.1007/s10661-006-9482-4.
- Ishaku, J.M., Ahmed, A.S. & M.A. Abubakar (2011). Assessment of groundwater quality using chemical indices and GIS mapping in Jada area, Northeastern Nigeria. *Journal of Earth Sciences Geotechnical Engineering*, 1(1), 35-60. Retrieved from: http://www.sciencpress.com/upload/geo/vol%201_1_3.pdf
- JICA (1999). El estudio de desarrollo integral de agricultura, ganadería y desarrollo rural de la región del Soconusco (Distrito de Desarrollo Rural No. 8, Tapachula) en Chiapas, Los Estados Unidos Mexicanos. Secretaría de Agricultura, Ganadería y Desarrollo Rural y Secretaría de Agricultura y Ganadería del Estado de Chiapas. Reporte Final. Tapachula, Chiapas. México: Agencia de Cooperación Internacional del Japón
- Joshi Dharendra Mohan, Alok Kumar & Namita Agrawal (2009). Assessment of the irrigation water quality of river Ganga in Haridwar District. *RASĀYAN J. Chem.*, 2(2), 285-292. Retrieved from: <http://www.rasayanjournal.co.in/vol-2/issue-2/7.pdf>
- Kankal, N., Indurkar, M., Gudadhe, S. & Wate, S. (2012). Water Quality Index of Surface Water Bodies of Gujarat, India. *Asian J. Exp. Sci.*, 26(1), 39-48.
- López Ramos. E. (1980) *Geología de México*. Tomo II. Segunda Edición. México, D.F., Published by the autor, 454 p.
- Macías, J. L., Arce, J. L., Garduño-Monroy, V. H., Rouwet, D., Taran, Y., Layer, P., ... & Álvarez, R. (2010). Estudio de prospección geotérmica para evaluar el potencial del volcán Chichonal, Chiapas. *Unpublished Report*, No. 9400047770.
- Mancilla, O. (2012). *Índices de Salinidad y Calidad de las aguas superficiales de Tlaxcala, Puebla y Veracruz*. (Tesis de Doctorado). Colegio de Posgraduados. Montecillo, México.
- Marín, L. E. (2002). Perspectives on Mexican Ground Water Resources. *Ground Water*, 40(6), 570-571. DOI: 10.1111/j.1745-6584.2002.tb02542.x.
- Miletto, M., Kirchheim, R., Rucks, J., Bello, E., Da Franca, N. & Dos Anjos, R. (2004). El recurso invisible Acuíferos transfronterizos: una oportunidad de cooperación internacional. *Series sobre elementos de Políticas*. 3. Washington, D.C.: Organización de Estados Americanos. Departamento de Desarrollo Sostenible y Medio Ambiente [en línea] Retrieved from: http://www.oas.org/dsd/policy_series/3_spa.pdf on 30/07/2014.
- Mohd, S., Hafizan, J., Sharifuddin, M. & Nur, H. (2011). Surface River Water Quality Interpretation Using Environmetric Techniques: Case Study at Perlis River Basin, Malaysia. *International Journal of Environmental Protection*, 1(5), 1-8. DOI 10.5963/IJEP0105001
- Mora-Chaparro, J. C., Carrera, M., García-Diego, A. M., Escobedo, S., Figueroa, H. N., Hernández, V. M., Sol, L. L. (2007). Reporte de observaciones geológicas en la ciudad de Tuxtla Gutiérrez, Chiapas, Informe técnico. Chiapas: Instituto de Protección Civil para el Manejo Integral de Riesgos de Desastre.
- Morán-Zenteno, D. (1994). The geology of the Mexican Republic. *American Association of Petroleum Geologists*, 1994 - 160 pp.
- Nag, S. K. & Ghosh, P. (2013). Variation in Groundwater Levels and Water Quality in Chhatna Block, Bankura District, West Bengal—A GIS Approach. *Journal of the Geological Society of India*, 81(2), 261-280. DOI 10.1007/s12594-013-0029-3
- Nagaraju, A., Suresh, S., Killham, K. y Hudson-Edwards, K. (2006). Hydrogeochemistry of Waters of Mangampeta Barite Mining Area, Cuddapah Basin, Andhra Pradesh, India. *Turkish Journal of Engineering Environmental Sciences*, 30(4), 203-219. Retrieved from: <http://journals.tubitak.gov.tr/engineering/issues/muh-06-30-4/muh-30-4-1-0406-2.pdf>
- Obiefuna, G.I. & Sheriff, A. (2011). Assessment of Shallow Ground Water Quality of Pindiga Gombe Area, Yola Area, NE, Nigeria for Irrigation and Domestic Purposes. *Research Journal of Environmental and Earth Sciences*, 3(2), 31-141. Retrieved from: <http://maxwellsci.com/print/rjees/v3-131-141.pdf>
- Olea, S. (2013). *Evaluación de la sustentabilidad hidrogeológica de los humedales del Soconusco, Chiapas*. (Tesis de Licenciatura). Facultad de Ingeniería. Universidad Autónoma de México, México.
- Palacios, O. & Aceves, E. (1970). *Instructivo para el registro, muestreo e interpretación de datos de calidad del agua para riego*. Colegio de Posgraduados. Serie de Apuntes No. 15. Chapingo, México.
- Papaioannou, A., Dovriki, E., Rigas, N., Plageras, P., Rigas, I., Kokkora, M. & Papastergiou, P. (2010). Assessment and Modelling of Groundwater Quality Data by Environmetric Methods in the Context of Public Health. *Water Resources. Management*, 24(12), 3257-3278.
- Peinado-Guevara, H.J., Green-Ruiz, C.R., Herrera-Barrientos, J., Escolero-Fuentes, O.A., Delgado-Rodríguez, O., Belmonte-Jiménez, S.I. &

- Ladrón M. (2011). Calidad y aptitud de uso agrícola y doméstico del agua del acuífero del río Sinaloa, porción costera. *Hidrobiológica*, 21(1), 63-76.
- Pérez-Sirvent, C., Martínez, M. & Sánchez, J. (2003). Efecto del riego con agua de mala calidad sobre la desertificación de zonas semi-áridas en Murcia, España. *Geoderma*, 113,109-125.
- Piper, A.M. (1944). A graphic procedure in the geochemical interpretation of water analysis. *EOS, Transactions American Geophysical Union*, 25(6), 914–928. DOI: 10.1029/TR025i006p00914
- Porta, J., López-Acevedo, M. & Poch, R. (2010). *Introducción a la Edafología: uso y protección de suelos*. (2a. ed.). Madrid, España: Mundi-Prensa.
- Price, M. (2003). *Agua subterránea*. (3a. ed.). México: Editorial Limusa México.
- Richards, L.A. (1954). Diagnosis and improvement of saline and alkali soils. *Soil Science*, 78(2), 154.
- Rodríguez, M., D'Urso, C., Rodríguez, G. & Sales, A. (2008). Evaluación de la Calidad de Aguas para Riego de la Cuenca del Río Calera, Tucumán, Argentina. *Ciencia*, 3(7),15-28.
- Romero, J. (2009). *Calidad del agua*. (3a. ed.). Bogotá, Colombia: Editorial Escuela colombiana de Ingeniería.
- Ruda, E., Mongiello, A., Acosta, A., Ocampo, E. & Contini, L. (2005). Calidad del agua subterránea con fines de riego suplementario en Argiudoles del Centro de Santa Fe, Argentina. *Agricultura Técnica*, 65(4), 411-420. DOI: <http://dx.doi.org/10.4067/S0365-28072005000400007>
- Salas G.P. (1980). Letter and provinces of the Mexican Republic. Council of Mineral Resources, 199 pp.
- Sharma, D. P. & Rao, K.V.G.K. (1998). Strategy for long term use of saline drainage water for irrigation in semi-arid regions. *Soil and Tillage Research*, 48(4), 287-295. DOI: [https://doi.org/10.1016/S0167-1987\(98\)00135-4](https://doi.org/10.1016/S0167-1987(98)00135-4)
- Todd, D.K. & Mays, L. (1980). *Groundwater Hydrology*. (3a. ed.). New York: Wiley International Edition.
- UNESCO (2007). Serie ISARM Américas. *Sistemas Acuiferos Transfronterizos en la Américas. Evaluación Preliminar*. Programa Hidrológico Internacional de la Oficina Regional de Ciencia para América Latina y el Caribe de la Organización de las Naciones Unidas para la Educación, la Ciencia y la Cultura. Departamento de Desarrollo Sostenible de la Organización de Estados Americanos. Serie 1. Montevideo, Uruguay. 178 pp.
- UNESCO (2010). PHI-VII/ Serie ISARM Américas. *Aspectos socioeconómicos, Ambientales y Climáticos de los Sistemas Acuiferos Transfronterizos de las Américas*. Oficina Regional de Ciencia para América Latina y el Caribe de la Organización de las Naciones Unidas para la Educación, la Ciencia y la Cultura. Departamento de Desarrollo Sostenible de la Organización de Estados Americanos. Serie 3. Montevideo, Uruguay. 544 pp.
- Wani, R.A., Mir A.H., Tanveer A., Jehangir A. & Yousuf A. (2014). Preliminary study on irrigational quality of some ground water sources of Kashmir, India. *International Journal of Scientific & Engineering Research*, 5(2), 318-323.
- Weber, B.L., Valencia, V.A., Schaaf, P., Pompa-Mera, V., Ruiz, J., 2008, Significance of provenance ages from the Chiapas Massif Complex (southeastern Mexico): Redefining the Paleozoic basement of the Maya Block and its evolution in a peri-Gondwanan realm: The Journal of Geology, 116, 619 639.
- Wijnen, M., Augeard, B., Hiller, B., Ward, C. & Huntjens, P. (2012). 71742. *Managing the invisible: Understanding and improving groundwater governance*. Washington, D. C.: Banco Mundial. Informe Preliminar. [en línea] Retrieved from: http://www-wds.worldbank.org/external/default/WDSContentServer/WDSP/IB/2012/08/09/000333037_20120809002923/Rendered/PDF/717420WP0Box370naging0the0invisible.pdf 10/07/2014
- Wilcox, L.V. (1955). Classification and Use of Irrigation Waters. *Circular 969*, Washington, D. C :United States Department of Agriculture. Retrieved from: <https://ia601701.us.archive.org/23/items/classificationus969wilc/classificationus969wilc.pdf>
- Yesilnacar, M.L. & Gulluoglu, M.S. (2008). Hydrochemical characteristics and the effects of irrigation on ground water quality in Harran plain, GAP project, Turkey. *Environmental Geology*, 54(1), 183-196.

Mean velocity and suspended sediment concentration profile model of turbulent shear flow with probability density function

Guanglin Wu^{a,b}, Liangsheng Zhu^{a,*}, Fangcheng Li^b

^aCollege of Civil and Transportation Engineering, South China University of Technology, Guangzhou 510641, China

^bCollege of Ocean Engineering, Guangdong Ocean University, Zhanjiang 524088, China

*Corresponding author. Tel: +86 02087111030-3682; E-mail: lshzhu@scut.edu.cn (L. S. Zhu)

ABSTRACT

This work purposes a general mean velocity and a suspended sediment concentration (SSC) model to express distribution in every point of the cross section of turbulent shear flow by using a probability density function method. In order to solve turbulent flow and avoid multifarious dynamical mechanics, the probability density function method was used to describe the velocity and concentration profiles interacted on directly by fluid particles in turbulent shear flow. The velocity profile model was obtained by solving for the profile integral with the product of the laminar velocity and probability density, through adopting an exponential probability density function to express probability distribution of velocity alteration of a fluid particle in turbulent shear flow. An SSC profile model was also created following a method similar to the above and based on the Schmidt diffusion equation. Different velocity and SSC profiles were created while changing the parameters of the models. The models were verified by comparing the calculated results with traditional models. It was shown that the probability density function model was superior to log-law in predicting stream-wise velocity profiles in coastal currents; and the probability density function SSC profile model was superior to the Rouse equation for predicting average SSC profiles in rivers and estuaries. Outlooks for precision investigation are stated at the end of this article.

Keywords: Exponential probability density; Mean velocity profile; Concentration profile; River flow; Coastal current

Velocidad media y modelo de perfil de concentración de sedimentos suspendidos de flujo turbulentos de cizalla turbulento con funciones de densidad de probabilidad.

RESUMEN

Este trabajo propone un modelo de velocidad media general y un modelo de concentración de sedimentos suspendidos (CSS) para expresar la distribución en cada punto de la sección de cruce del flujo turbulento de cizalla mediante el uso de funciones de densidad de probabilidad (PDF). El método de funciones de densidad de probabilidad se usó para describir los perfiles velocidad y concentración que interactuaron directamente con partículas fluidas en el flujo de desprendimiento turbulento para resolver el flujo turbulento y evitar diferentes mecánicas dinámicas. El modelo del perfil de velocidad se obtuvo resolviendo el perfil integral con el producto de la velocidad laminar y la densidad de probabilidad, mediante la adopción de una función de densidad exponencial para expresar la probabilidad de distribución de la velocidad de alteración de la partícula de un fluido en un flujo de desprendimiento turbulento. También se creó un modelo de perfil CSS siguiendo un método similar al anterior y basado en la ecuación de difusión Schmidt. Se crearon diferentes perfiles de velocidad y CSS durante el cambio de parámetros de los modelos. Los modelos se verificaron comparando los resultados calculados con los modelos tradicionales. Se demostró que el PDF era superior a la ley logarítmica en la predicción de los perfiles de velocidad en corrientes costeras, y que la probabilidad del modelo del perfil de función de densidad SSC fue superior a la ecuación Rouse para predecir perfiles SSC promedio en ríos y estuarios. Las perspectivas para la investigación de precisión se indican al final de este artículo.

Palabras clave: densidad de probabilidad exponencial, perfil de velocidad media, perfil de concentración, corriente de río, corriente costera.

Record

Manuscript received: 22/05/2017

Accepted for publication: 23/08/2017

How to cite item

Wu, G., Zhu, L., & Li, F. (2017). Mean velocity and suspended sediment concentration profile model of turbulent shear flow with probability density function. *Earth Sciences Research Journal*, 21(3), 129 - 134.

doi: <http://dx.doi.org/10.15446/esrj.v21n3.65172>

Introduction

Turbulence is much more complex than laminar flow. According to the Boussinesq eddy viscosity assumption (Boussinesq, 1877), the logarithmic law for velocity profile was solved by using the mixing length method (Prandtl, 1925; Khan et al., 2017; Zawar et al., 2017). Some vertical velocity distribution laws, such as the power law and the exponential law, are based on experimental considerations or semi-empirical theories (Lin et al., 1953; Deissler, 1954; Afzal et al., 2007). Other laws for turbulent velocity profile or concentration profile are based on an indirect turbulence model (Bucci et al., 2008; Nucci and Fiorucci, 2011).

Logarithm law is the most popular one used to express the mean velocity in a cross section of turbulent flow for wind flow, river flow, and lake models. The logarithm law fits velocity and concentration distribution in the position far away from the interface in developed turbulent flow (Wang and Yu, 2007). Some researchers have focused on mean velocity profiles of turbulent wall-bounded flows separately (Poggi et al., 2002; Buschmann and Gad-el-Hak, 2007; Kempe et al., 2007; Buschmann et al., 2009).

Different vertical velocity distribution laws are used to describe stream-wise velocity structure in coastal currents (Soulsby, 1980; Anwar, 1996, 1998; De Serio and Mossa, 2014), in tidal channels (Soulsby and Dyer, 1981), and on the continental shelf (Soulsby, 1983; De Serio and Mossa, 2010). Vertical distribution of suspended sediment concentration (SSC) in rivers, estuaries, and coastal currents have been studied by many researchers through the years (Rouse, 1937; Taylor and Dyer, 1977; Li et al., 2014). This work derives general formulas to describe the mean velocity and SSC distributions of turbulent shear flow to fit the whole cross section from the bottom boundary to the upper boundary, using a probability density function method.

A brief review of classical methods for velocity profile of shear flow

Consider the laminar shear flow—the steady incompressible developed flow between two interfaces, with one interface moving with velocity U and the other being motionless. The flow can be solved based on 2-dimensional Navier-Stokes equations and expressed as

$$\frac{u(y)}{U} = \frac{y}{h} - \frac{h^2}{2\mu U} \frac{dp}{dx} \frac{y}{h} \left(1 - \frac{y}{h}\right) \quad (1)$$

Here h is the distance between two interfaces, μ is dynamic viscosity, and dp/dx is the pressure gradient along the x -direction. The velocity profile of shear flow can be simplified to Eq. (2) when $dp/dx = 0$

$$\frac{u(y)}{U} = \frac{y}{h} \quad (2)$$

Logarithm law (Prandtl, 1925), derived by the mixing length method, is the most popular equation used to express the mean velocity in a cross section of turbulent shear flow. The basic logarithm law of mean velocity profile of turbulent shear flow is

$$\frac{\bar{u}(y)}{u_*} = \frac{1}{\kappa} \ln \frac{y}{h} + \frac{1}{\kappa} \ln \frac{u_* h}{\nu} + \frac{1}{\kappa} \ln \frac{\nu}{u_* y_0} = \frac{1}{\kappa} \ln \frac{y}{h} + B' \quad (3)$$

Here, u_* is the shear velocity of the fluid and y_0 is hydrodynamic roughness length. But Eq. (3) cannot fit select velocity profiles not full profiles because of the assumption that the mixing length is proportional to the distance away from the wall boundary. Many instances and experiments have proven that the mixing length method can successfully predict velocity distributions far away from the interfaces, but it cannot predict velocity distribution near interfaces such as walls, seabed, gas-liquid surfaces, and so on.

As far as we know, turbulent intensity should be dependent on the Reynolds number, which is composed of the characteristic velocity, characteristic length, and kinematic viscosity. Considering the mixing length method carefully, the core assumption is that the eddy viscosity is in direct proportion to the average velocity gradient and the mixing length is in direct proportion to the distance away from the wall. The method does not directly create the relationship between turbulent parameters and average velocity.

Exponential probability density model (EPDM) for mean velocity profile of turbulent shear flow

To solve for turbulent flow without closely associated different dynamical mechanics, a probability density function method is adopted to describe the pulsating intensity of velocity of fluid particles in this study. The pulsating intensity of every fluid particle in the profile will impact the whole profile. The effect decays at a distance from its original position and obeys a probability density function. Exponential probability density function is often used to describe the decay degree distribution in many physical and chemical problems. In many situations, the exponential probability density function model is an appropriate method to approach the random decay phenomena. The primary expression of the exponential probability density function is

$$p(y) = \lambda e^{-\lambda|\Delta y|} \quad (4)$$

Here, $p(y)$ is the probability density of a fluid particle impacting any position, λ is the damping index, and y is the distance from the particle position y_i to the impacting position y , defined by

$$\Delta y = y - y_i \quad (5)$$

As shown in Fig. 1, the expression of exponential probability density function $p_1(y)$, represents the probability density that the velocity of laminar shear flow at position y_1 , u_1 , distributes to any position y due to turbulence. Because the expression satisfies the boundary condition that $p_1(y_1) = p_{m1}$ where $y = y_1$ as shown in Fig. 1, $\lambda = p_m$, such as $\lambda_1 = p_{m1}$, $\lambda_2 = p_{m2}$, and so on. Hence, the expression $p_i(y)$ satisfies

$$p_i(y) = p_{mi} e^{-p_{mi}|y-y_i|} \quad (6)$$

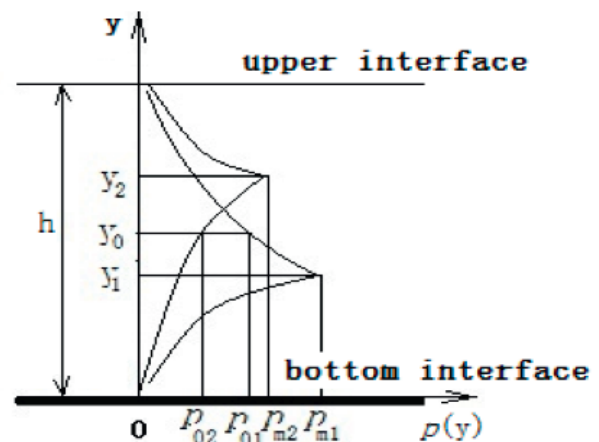


Figure 1. Schematic diagram of exponential probability density for pulsating intensity transfer

The probability density of u , velocity of any position of y , distributes to y_0 , a certain position at the profile, is defined as p_0 as shown in Fig. 1, such as p_{01} and p_{02} . We have

$$p_{0i} = p_i(y_0) = p_m(y) e^{-p_m(y)|y_0-y|} \quad (7)$$

average turbulent velocity of a particular position, y_0 , produced by integrating the product of the local laminar velocity in Eq. (7), which is solved with Navier-Stokes equations, and the exponential probability density function of pulsating intensity at the position, across all fluid particles in the profile, is shown as

$$\bar{u}(y_0) = \int_0^h \alpha u(y) p_i(y_0) dy \quad (8)$$

Here α is an adjustment.

Substituting $u(y)$ with Eq. (2) and $p_0(y)$ with Eq. (7) in Eq. (8), we get

$$\frac{\bar{u}(y_0)}{U} = \alpha \int_0^h \frac{y}{h} p_m(y) e^{-p_m(y)|y_0-y|} dy \quad (9)$$

Eq. (9) cannot be analytically and fully solved. To solve Eq. (8), we assume that

$$p_i(y_0) = p_0(y) = p_{m0} e^{-p_{m0}|y-y_0|} \quad (10)$$

Substituting Eq. (2) and Eq. (10) into Eq. (8), the result is

$$\frac{\bar{u}(y_0)}{U} = \alpha \int_0^h \frac{y}{h} u(y) p_{m0} e^{-p_{m0}|y-y_0|} dy \quad (11)$$

Integrating Eq. (11), the result is

$$\frac{\bar{u}(y_0)}{\alpha U} = \int_0^{y_0} \frac{y}{h} p_{m0} e^{p_{m0}(y-y_0)} dy + \int_{y_0}^h \frac{y}{h} p_{m0} e^{p_{m0}(y_0-y)} dy = \frac{e^{-p_{m0}y_0}}{p_{m0}h} - \left(\frac{1}{p_{m0}h} + 1 \right) e^{p_{m0}h(y_0/h-1)} + 2 \frac{y_0}{h} \quad (12)$$

Setting

$$P = p_{m0}h \quad (13)$$

and substituting y_0 with y in Eq.(12), the velocity profile of turbulent shear flow with this method (called PDFM) should be

$$\frac{\bar{u}(y)}{\alpha U} = \frac{e^{-P\frac{y}{h}}}{P} - \left(\frac{1}{P} + 1 \right) e^{P\left(\frac{y}{h}-1\right)} + 2 \frac{y}{h} \quad (14)$$

Assume that

$$P = p_m(y)h = m\left(\frac{y}{h}\right)^n \quad (15)$$

Eq. (14) can be calculated when the adjustable parameters, m and n , are given.

The mean turbulent velocity in Eq. (14) can be calculated by giving different m and n , as well as defining the dimensionless turbulent velocity and dimensionless position as

$$\bar{u}^+ = \bar{u}(y)/\bar{u}(h), \quad y^+ = y/h \quad (16)$$

The calculated results are shown in Fig. 2 and Fig. 3. Fig. 2 reveals that the mean velocity profile changes when the value of m is changed, but the mean velocity changes are weaker in the region near the wall or other interfaces than in the intermediate region while $\alpha=1$. The dimensionless velocities are almost the same in the region when the value of y^+ is between 0 and 0.25, but they change very evidently near the position where y^+ is approximately equal to 0.8. Thus, the upper mean velocity will increase along with an increasing value of m . The curve shape fits turbulent velocity profile when the value of m is lower in this case, such as $m=0.25, 0.1$ and 0.01 .

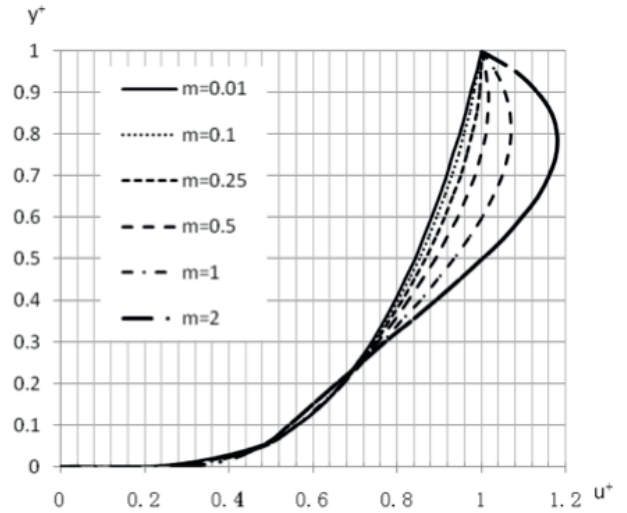


Figure 2. Mean velocity profiles with change of m ($n = 0.25$)

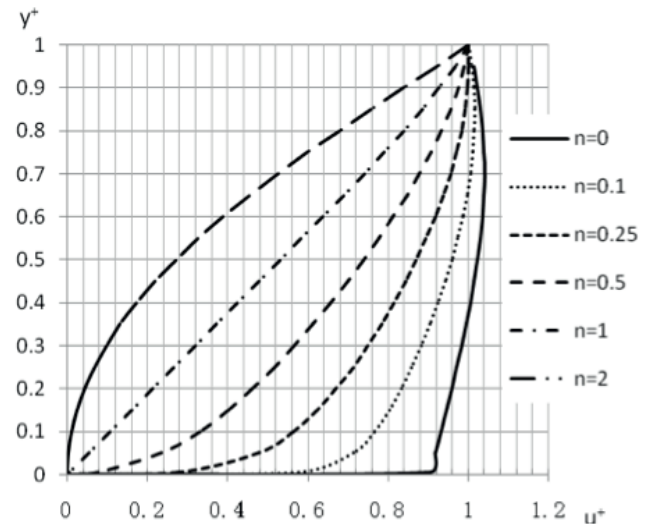


Figure 3. Mean velocity profiles with change of n ($m = 0.3$)

The mean velocity profiles are distinct when the values of n are different, as shown in Fig. 3, while $\alpha=1$. The main tendency of the profile curves is shifting from the top left to the bottom right in Fig. 3 along with the decreasing value of n . The tendency indicates that the parameter n has a closed relationship with turbulent intensity.

Verification of PDFM in coastal currents

The mean velocity profile model derived in the previous section was applied to fit the investigated profiles to verify the effectiveness of the model. To use Eq. (14) conveniently, the profile formula of PDFM should be transformed as

$$\frac{\bar{u}(y)}{u^*} = \beta \left(\frac{e^{-p\frac{y}{h}}}{P} - \left(\frac{1}{P} + 1 \right) e^{P(y/h-1)} + 2\frac{y}{h} \right) \quad (17)$$

Here $\beta = \alpha U/u^*$.

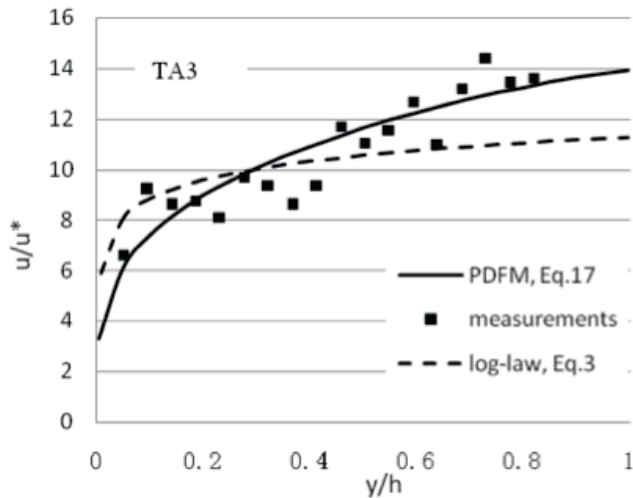
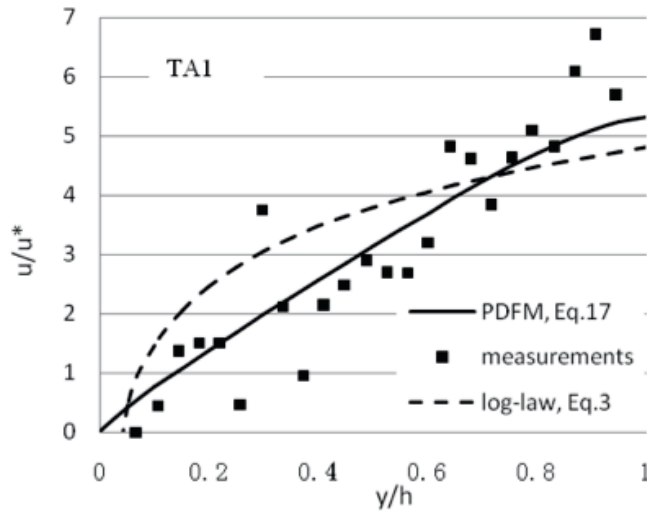


Figure 4. Calculated and measured vertical profiles of the stream-wise velocity of coastal currents at Taranto (Survey data cited in De Serio and Mossa (2014))

De Serio and Mossa (2010, 2014) investigated vertical profiles of the stream-wise velocity of the coastal currents at the Taranto (TA) and Bari (BA) sites in Italy. The comparison between the measurement data, the log law as shown in Eq. (3), and the PDFM as shown in Eq. (17) is plotted in Fig. 4 at Taranto for vertical stream-wise velocity profiles in shallow coastal currents. The calculated results show that the probability density function model (PDFM) more accurately reflects measurement data than the log-law model.

SSC profiles model and its verification in river and estuary

The Rouse equation (Rouse, 1937) was the most popular method used to calculate vertical concentration profiles of suspended load in rivers, lakes, estuarine and coastal currents, as well as on the continental shelf. The Rouse formula was

$$\frac{\bar{C}(y)}{C_a} = \left(\frac{y_a h - y}{y h - y_a} \right)^{z^*} \quad (18)$$

in which y_a is the thickness of the sheet-flow layer, C_a is the concentration at y_a which equals the bed-load concentration, $z^* = \omega/\kappa u^*$ is the suspension index, and ω is the particle settling velocity. The similar expression of PDFM also can be created by the method below based on the Schmidt diffusion equation (Schmidt, 1925).

$$\omega \bar{C}(y) + \varepsilon d\bar{C}(y)/dy = 0 \quad (19a)$$

That is

$$\frac{d\bar{C}(y)}{\bar{C}(y)} = \frac{-\omega}{\varepsilon} dy \quad (19b)$$

in which ε is the particle diffusion coefficient, set as an assumption of the exponential probability density function

$$\varepsilon = \varepsilon_0 e^{\varepsilon_0(y/h-1)} \quad (20)$$

then

$$\frac{d\bar{C}(y)}{\bar{C}(y)} = \frac{-\omega}{\varepsilon_0} e^{\varepsilon_0(1-y/h)} dy \quad (21)$$

Hence,

$$\frac{\bar{C}(y)}{C_a} = e^{\frac{\omega \varepsilon_0^h}{\varepsilon_0^2} (e^{-y/h} - 1)} = e^{\gamma(e^{-y/h} - 1)} \quad (22)$$

Here γ is the suspension index of this model.

The results of SSC profiles calculated on PDFM of Eq. (22) are shown in Fig. 5.

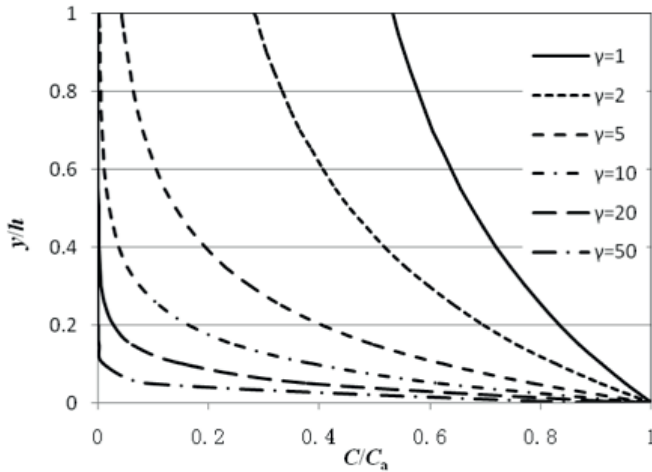


Figure 5. Calculated results of suspended sediment concentration profile model

Figure 5 shows that the slope of the profile curves is bigger near the surface than the bottom and the upper slope increases as the lower slope decrease when γ is increasing. The trend means that the particle settling velocity, particle diffusion coefficient and the water depth velocity influence γ to change the SSC distribution in the vertical cross section.

The SSC is very small when $\gamma=50$, so the bed load is the dominant composition when $\gamma \geq 50$. The curves also show that the SSC at surfaces is greater than zero when $\gamma \leq 2$. On the contrary, the SSC at surfaces tends to zero when $\gamma > 2$. So, this model provides an approach to avoid the surface limitation of Rouse equation.

Zhang et al. (2007) investigated SSC of the Yangtze River in detail and concluded a semi-empirical model of SSC. A comparison of predicting profiles between the PDFM (Eq. 22) and the Rouse equation [Eq. (18)] with the measurements in the Yangtze River is shown in Fig. 6. As shown in the figure, the PDFM model used for this study more accurately reflects the measurement data than does the Rouse equation.

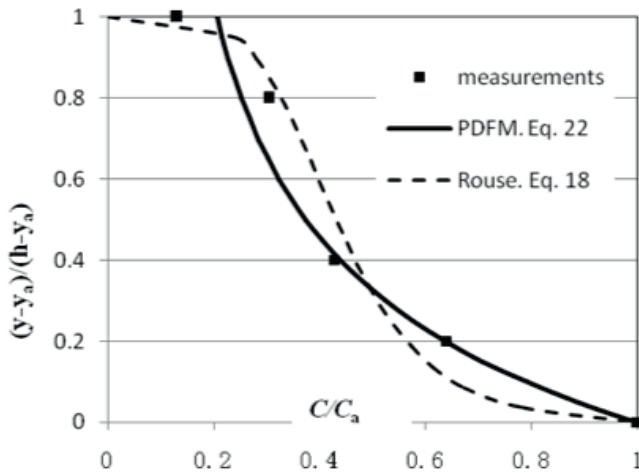


Figure 6. Calculated and measured vertical SSC profile in the Yangtze River (Survey data cited in Zhang et al. (2007))

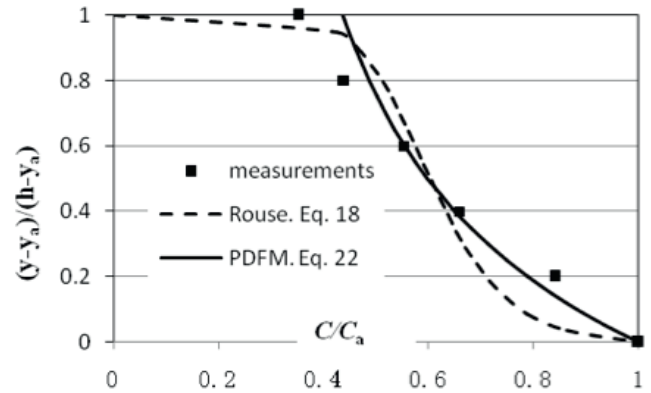


Figure 7. Calculated and measured vertical SSC profile in the Yangtze Estuary (Survey data cited in Liu, et al. (2014))

Liu, Yang, Zhu, et al. (2014) investigated the average SSC profile in the Yangtze Estuary in detail. The survey data is cited here to verify the PDFM model, Eq. (22). The comparison between the Rouse equation, PDFM, and measurements is shown in Fig. 7. The PDFM model of this study is also agreed more closely with the measurement data than does the Rouse equation in the case of the estuarine area.

Discussions

A model for solving velocity and concentration distribution of turbulent flow by using probabilistic methods is put forward in the article (Khan et al., 2017; Sultana et al., 2017). General models for describing the mean velocity and SSC profiles of a whole cross section in turbulent shear flow are derived based on the idea. In fact, the velocity profile formula of laminar shear flow is also the mean velocity profile solution of turbulent flow which ignores the turbulent items in Reynolds equation, thus the pulsating intensity of fluid particles is apparently related to it. On the other hand, the pulsating intensity is also under the control of certain boundary conditions. The exponential probability density function may describe the pulsating intensity of fluid particles of the whole cross section correctly to study mean velocity and concentration distributions. The calculated results of the derived formulas are as diverse as the changing the damping index of exponential probability density function. An innovative approach may be found to solve complex turbulent flow by expanding on this concept.

Conclusions

The PDFMmodel of this study possesses some advantage in the fields of predicting stream-wise velocity profiles of coastal currents and SSC profiles in river and estuaries as shown in the previous examples. Further research is needed to validate the method through continued studies and carried forward to clarify and optimize the parameters of these models to apply for practical problems. For advanced research, the parameters should be studied meticulously, such as its relationship with dynamic parameters, particularly turbulent characteristic parameters.

Acknowledgments

This work was partially supported by the Guangdong Province Science and Technology Research Project (2010B030600007) and Projects of Enhancing School with Innovation of Guangdong Ocean University (GDOU2016050258 & GDOU2017052503).

References

- Afzal, N., Seena, A., & Bushra, A. (2007). Power law velocity profile in fully developed turbulent pipe and channel flows. *Journal of Hydraulic Engineering*, 133(9), 1080-1086.
- Anwar, H. O. (1996). Velocity profile in shallow coastal water. *Journal of Hydraulic Engineering*, 122 (4), 220-223.
- Anwar, H. O. (1998). Spread of Surface Plume in Homogeneous and Stratified Coastal Waters. *Journal of Hydraulic Engineering*, 124 (5), 465-473.
- Boussinesq, J. (1877). *Essai sur la Théorie des Eaux Courantes*. Académie des Sciences. (Essay on the Theory of Water Flow. In French). French Academy of Sciences 23(1), 666-680.
- Bucci, G., Fiorucci, E., Russo, S. A., & Nucci, C. D. (2008). Analysis of turbulent flow speed profiles in pressure pipes using the dissimilar similitude technique applied to an electrolytic tank: implementation and experimental characterization. *IEEE Transactions on Instrumentation and Measurement*, 57(8), 1547-1553.
- Buschmann, M. H. & Gad-el-Hak, M. (2007). Recent developments in scaling of wall-bounded flows. *Progress in Aerospace Sciences*, 42(5), 419-467.
- Buschmann, M. H., Indinger, T., & Gad-el-Hak, M. (2009). Near-wall behavior of turbulent wall-bounded flows. *International Journal of Heat and Fluid Flow*, 30 (5), 993-1006.
- De Serio, F., & Mossa, M. (2010). *Velocity profiles of sea currents*. In: Proceedings of the 6th International Symposium on Environmental Hydraulics, Athens, Greece, 23-25 June 2010, CRC Press, 451-456.
- De Serio, F. & Mossa, M. (2014). Stream-wise velocity profiles in coastal currents. *Environmental Fluid Mechanics*, 14(4), 895-918.
- Deissler, R. G. (1954). *Analysis of turbulent heat transfer, mass transfer and friction in smooth tubes at high Prandtl and Schmidt*. National Advisory Committee for Astronauts, Washington D.C., USA.
- Kempe, A., Schlamp, S., & Rösger, T. (2007). Non-contact boundary layer profiler using low-coherence self-referencing velocimetry. *Experiments in Fluids*, 43(2-3), 453-461.
- Khan, M. Z., Rahman, Z. U., Khattak, Z., & Ishfaq, M. (2017). Microfacies and Diagenetic Analysis of Chorgali Carbonates, Chorgali Pass, Khair-E-Murat Range: Implications for Hydrocarbon Reservoir Characterization. *Pakistan Journal of Geology*, 1(1): 18-23.
- Lin, C. S., Moulton, R. W., & Putnam, G. L. (1953). Mass transfer between solid wall and fluid streams, mechanism and eddy distribution relationships in turbulent flow. *Industrial and Engineering Chemistry*, 45(3), 636-640.
- Liu, J. H., Yang, S. L., Zhu, Q., & Zhang, J. (2014). Controls on suspended sediment concentration profiles in the shallow and turbid Yangtze Estuary. *Continental Shelf Research*, 90(1), 96-108.
- Nucci, C. D., & Fiorucci, E. (2011). Mean velocity profiles of fully-developed turbulent flows near smooth walls. *Comptes Rendus Mécanique*, 339(6), 388-395.
- Poggi, D., Porporato, A., & Ridolfi, L. (2002). An experimental contribution to near-wall measurements by means of a special laser Doppler anemometry technique. *Experiments in Fluids*, 32(3), 366-375.
- Prandtl, L. (1925). Über die ausgebildete Turbulenz. (On Fully Developed Turbulence. In German). *Z.A.M.M.*, 5, 136-139.
- Rouse, H. (1937). Modern conceptions of the mechanics of fluid turbulence. *Trans. ASCE*, 102(1), 463-543.
- Schmidt, W. (1925). XXIII. Gefügestatistik. *Zeitschrift für Kristallographie. Mineralogie und Petrographie*, 38(1), 392-423.
- Soulsby, R. L. (1980). Selecting record length and digitization rate for near-bed turbulence measurements. *Journal of Physical Oceanography*, 10(2), 208-219.
- Soulsby, R. L. (1983). *The bottom boundary layer of shelf seas*. Physical Oceanography of Coastal and Shelf seas ed., Elsevier oceanography series 35, 189-266.
- Soulsby, R. L., & Dyer, K. R. (1981). The form of the near-bed velocity profile in a tidally accelerating flow. *Journal of Geophysical Research: Oceans*, 86(C9), 8067-8074.
- Sultana, M. N., Akib, S., & Ashraf, M. A. (2017). Thermal comfort and runoff water quality performance on green roofs in tropical conditions. *Geology, Ecology, and Landscapes*, 1(1), 47-55.
- Taylor, P. A., & Dyer, K. R. (1977). The theoretical models of flow near the bed and their implication for sediment transport. *The Sea*, 6(1), 579-601.
- Wang, Y. H., & Yu, G. H. (2007). Velocity and concentration profiles of particle movement in sheet flows. *Advances in water resources*, 30(5), 1355-1359.
- Zawar, Z. U., Khan, M., Khattak, Z., Abbas, M. A., & Ishfaq, M. (2017). Microfacies Analysis and Reservoir Potential of Sakesar Limestone, Nammal Gorge (Western Salt Range), Upper Indus Basin, Pakistan. *Pakistan Journal of Geology*, 1(1), 12-17.
- Zhang, R. J., Xie, J. H., Chen, & W. B. (2007). *River dynamics* (In Chinese). Wuhan Univ. Press, Wuhan, Hubei, P.R. China.

Online Outlier Detection for Time-varying Time Series on Improved ARHMM in Geological Mineral Grade Analysis Process

Jianjun Zhao^{a,b}, Junwu Zhou^b, Weixing Su^c, Fang Liu^c

^a School of Information Science & Engineering, Northeastern University, Shenyang 110004, China;

^b BeiJing General Research Institute of Mining & Metallurgy, BeiJing 100160, China

^c School of Computer Science & Software Engineering, Tianjin Polytechnic University, Tianjin 300387, China

*Email of Corresponding Author: 15900201597@163.com

ABSTRACT

Given the difficulty of accurate online detection for massive data collecting real-timely in a strong noise environment during the complex geological mineral grade analysis process, an order self-learning ARHMM (Autoregressive Hidden Markov Model) algorithm is proposed to carry out online outlier detection in the geological mineral grade analysis process. The algorithm utilizes AR model to fit the time series obtained from "Online x-ray Fluorescent Mineral Analyzer" and makes use of HMM as a basic detection tool, which can avoid the deficiency of presetting the threshold in traditional detection methods. The structure of traditional BDT (Brockwell-Dahlhaus-Trindade) algorithm is improved to be a double iterative structure in which iterative calculation from both time and order is applied respectively to update parameters of ARHMM online. With the purpose of reducing the influence of outlier on parameter update of ARHMM, the strategies of detection-before-update and detection-based-update are adopted, which also improve the robustness of the algorithm. Subsequent simulation by model data and practical application verify the accuracy, robustness, and property of online detection of the algorithm. According to the result, it is obvious that new algorithm proposed in this paper is more suitable for outlier detection of mineral grade analysis data in geology and mineral processing.

Keywords: ARHMM; BDT; KICvc; outlier detection; online detection.

Detección en tiempo real de valores atípicos sobre series de tiempo variable en ARHMM mejorado durante el proceso de análisis de grado mineralógico

RESUMEN

Existe gran dificultad para la detección en tiempo real para series de datos masivos con altos niveles de ruido de valores atípicos. Se propone un algoritmo de autoaprendizaje ARHMM (Modelo autoregresivo oculto de Markov) para llevar a cabo la detección de dichos valores atípicos en el proceso de análisis del grado mineral geológico. El algoritmo usa un modelo AR para ajustar la serie de tiempo obtenida del "analyzer de fluorescencia de rayos X" y hace uso del HMM como una herramienta básica de detección, la cual puede evitar la deficiencia de predeterminedar el umbral en métodos tradicionales de detección. Para actualizar los parámetros del ARHMM en tiempo real, la estructura del algoritmo BDT (Brockwell-Dahlhaus-Trindade) tradicional se mejora para ser una doble estructura iterativa en la que se aplica el cálculo iterativo en tiempo y en orden respectivamente. Con el propósito de reducir la influencia de valores atípicos (o extremos) en la actualización del parámetro de ARHMM, se adoptan las estrategias de detección-antes-que-actualización y la detección-basada-en-actualización, lo que también aumenta la robustez del algoritmo. La subsiguiente simulación por modelos de datos y aplicación práctica comprueba la precisión, fortaleza y capacidad de la detección en línea del algoritmo. De acuerdo con el resultado, es evidente que el nuevo algoritmo propuesto en este artículo es más apropiado para la detección de datos de valores atípicos para el análisis del grado mineral en geología y el procesamiento mineral.

Palabras clave: Modelo autoregresivo oculto de Markov; detección en tiempo real; Brockwell-Dahlhaus-Trindade.

Record

Manuscript received: 21/02/2017

Accepted for publication: 28/07/2017

How to cite item

Zhao, J., Zhou, J., Su, W., & Liu, F. (2017). Online Outlier Detection for Time-varying Time Series on Improved ARHMM in Geological Mineral Grade Analysis Process. *Earth Sciences Research Journal*, 21(3), 135-139.

doi: <http://dx.doi.org/10.15446/esrj.v21n3.65215>

Introduction

Mineral composition analysis is a key factor in determining whether or not to carry out mining. Over the years, many scholars have proposed some new ideas and methods for accurate mineral grade assessment, many of which are based on chemical or physical test equipment to obtain the data for ingredient grade analysis (Kameshwara, Rao, & Narayana, 2014; De'nan, Naaim, & Leong, 2017). Therefore, the accuracy of the data used for ore composition analysis is critical to the ore grade analysis. At present, automated testing equipment is used in ore grade analysis, such as "BOX-A type on-stream x-ray fluorescence analyzer", which uses spectral obtain by irradiating X-rays to the pulp to get the results of ore grade. It is worth noting that BOX-A type on-stream x-ray fluorescence analyzer by default is that the spectral data obtained is correct. But whether it is chemical or physical testing equipment are inevitably produced abnormal data. Those outliers directly affect the analysis results of the mineral products analyser (Clarke, & Levis, 1998; Rivoirard, Demange, & Freulon, 2013). Therefore, the detection and elimination of these abnormal data is the premise and key to the above ore grade analysis work.

A new algorithm is proposed here to especially do outlier detection for ore inspection data which obtain from chemical or physical testing equipment. The algorithm utilizes AR model to fit the time series and makes use of HMM as a basic detection tool, which can avoid the deficiency of presetting the threshold in traditional detection methods. To update parameters of ARHMM online, the structure of traditional BDT (Brockwell-Dahlhaus-Trindade) algorithm is improved here, and a double iterative structure in which iterative calculation from both time and order is applied respectively. With the purpose of reducing the influence of outlier on parameter update of ARHMM, the strategies of detection-before-update and detection-based-update are adopted, which also improve the robustness of the algorithm. Subsequent simulation by model data and practical application verify the accuracy, robustness, and property of online detection of the algorithm.

In this paper our innovations are shown as follow:

1. Unlike other outlier detect method (such as the traditional AR model detection method), the outliers detect method proposed in this paper does not need to set the detection threshold.
2. Considering the problem that the model order of chemical or physical testing equipment's hard to be determined, the new detected method which is based on residual error has the function of model order self-learning.
3. In a view to avoid the influence of outliers on the test results, this paper proposes a detection-before-update and detection-based-update strategies.

The Predecessors' Achievements on Outlier detection

Many good ideas and methods are put forward for the research of outliers detection problem, such as that Barnett and Lewis proposed an outliers detected method based on statistics in their word named 'Outlier in Statistical Data (Barnett & Lewis, 1994). Outlier detection method based on distance is proposed by Knorr and Raymond (Knorr & Ng, 1999; Edwin & Raymond, 1998), an new detected method based on density is suggested by Ramaswamy et al. (2000). But for ore inspection data, the detection methods based on distance, density or variance is a lack of feasibility since an online real-time detection method be needed for the ore test data. With the research of anomaly data detection technology, many new ideas and techniques are introduced, such as clustering analysis (Almeida & Barbosa, 2007) and neural network method (Bullen, Cornford, & Nnbney, 2003; Prakobphol, & Zhan, 2008). But clustering analysis method is also not suitable for online outlier detection for extensive test data, and neural network method requires a lot of data to model learning. In 1995, Ragaran and Argrawal put forward the concept of "sequence anomaly" (Han & Micheline, 2001) and proposed the detection method based on deviation (Takeuchi, & Yamanishi, 2006). Because this method needs to know the order of the model, it can not be directly used for the outlier detection of mineral grade analysis data.

Structure of Double iteration in BDT

To make the BDT algorithm can be calculated online, the improved BDT algorithm with double repetition structure is proposed in this paper.

Traditional BDT algorithm

The traditional BDT algorithm is improved by Levinson-Durbin algorithm which is proposed by Brockwell et al. (2002). For traditional BDT algorithm, using all the data to the iterative calculation of model order, in a view to obtain the order of the forward and backward AR model.

$x_t, t=1,2,\dots$ is the test data waiting for detection, where x_t is m -dimension vectors. So forward AR model can be express as Equation 1.

$$x_t = \sum_{i=1}^k a_k(i)x_{t-i} + \varepsilon_k(t) \quad (1)$$

In which, $\varepsilon_k(t)$ is forward residual under k order model, which obeys Gauss distribution with zero means. $a_k(i)$ is the coefficient of forwarding AR model under k order model. So backward AR model can be written as Equation 2.

$$x_t = \sum_{j=1}^k b_k(j)x_{t+j} + \eta_k(t) \quad (2)$$

With Minimizing all data forward and backward residual as the target, so the generalized objective function written as Equation 3 (Trindade, 2003).

$$\min \sum_{t=k+1}^n [\hat{\varepsilon}_k(t)' \omega_1 \hat{\varepsilon}_k(t) + \hat{\eta}_k(t-k)' \omega_2 \hat{\eta}_k(t-k)] \quad (3)$$

n is the number of the data. ω_1 and ω_2 are weighted coefficient matrix for forwarding and backward AR model, and in BDT algorithm, the values of ω_1 and ω_2 is 1. $\hat{\varepsilon}_k(t)$ and $\hat{\eta}_k(t-k)$ are Estimated residual values for forward and backward AR model individually.

$$\hat{\varepsilon}_k(t) = x_t - \sum_{i=1}^k a_k(i)x_{t-i} \quad (4)$$

$$\hat{\eta}_k(t-k) = x_{t-k} - \sum_{j=1}^k b_k(j)x_{t-k+j} \quad (5)$$

In which, $a_k(i), i=1,2,\dots,k$, $b_k(j), j=1,2,\dots,k$ are m -dimension matrix. The traditional BDT algorithm can be written in full as followed:

$$a_k(k) = \left(\frac{1}{n} \sum_{t=1}^{n+k} \hat{\varepsilon}_{k-1}(t) \hat{\eta}_{k-1}(t-k) \right) \hat{V}_{k-1}^{-1} \quad (6)$$

$$a_k(i) = a_{k-1}(i) - a_k(k) b_{k-1}(k-i), \quad i = 1, \dots, k-1 \quad (7)$$

$$b_k(k) = \hat{V}_{k-1}^{-1} a_{k-1}(k) \hat{U}_{k-1}^{-1} \quad (8)$$

$$b_k(j) = b_{k-1}(j) - b_k(k) a_{k-1}(k-j), \quad j = 1, 2, \dots, k-1 \quad (9)$$

$$\hat{U}_k = \hat{U}_{k-1} - a_k(k) \hat{V}_{k-1}^{-1} a_k(k)' \quad (10)$$

$$\hat{V}_k = \hat{V}_{k-1} - b_k(k) \hat{U}_{k-1}^{-1} b_k(k)' \quad (11)$$

$$\hat{\varepsilon}_k(t) = \hat{\varepsilon}_{k-1}(t) - a_k(k) \hat{\eta}_{k-1}(t-k) \quad (12)$$

$$\hat{\eta}_k(t) = \hat{\eta}_{k-1}(t) - b_k(k) \hat{\varepsilon}_{k-1}(t+k) \quad (13)$$

In Equation 6 to Equation 13, \hat{U}_k and \hat{V}_k are estimated variance for forwarding and backward noise. The initial condition for traditional BDT algorithm are:

$$\hat{\varepsilon}_k(t) = \hat{\eta}_k(t) = \begin{cases} x_t, & t \in \{1, 2, \dots, n\} \\ 0, & \text{others} \end{cases} \quad (14)$$

$$\hat{U}_\phi = \hat{\Gamma}(0) = \hat{V}_\phi \quad (15)$$

$$\hat{\Gamma}(0) = \frac{1}{n} \sum_{t=1}^n x_t x_t' \quad (16)$$

The subscript ϕ express that when the initial iteration, the model order set is empty.

• Double iteration BDT algorithm

The objective function of improved BDT algorithm also is Equation 3. The dynamic performance of the algorithm is enhanced by the forgetting factor. The improved BDT algorithm has double loop structure which model order is inner loop and time is the outer loop.

We set $R_k = \frac{1}{n} \sum_{t=1}^{n+k} \hat{\epsilon}_{k-1}(t) \hat{\eta}_{k-1}(t-k)$, which is part of Equation 6. So:

$$R_i = \frac{1}{n} \sum_{t=1}^{n+i} \hat{\epsilon}_{i-1}(t) \hat{\eta}_{i-1}(t-i), i = 1, 2, \dots, k, \dots, K \quad (17)$$

In Equation 7, k a set maximum value for model order. Considering the time-varying characteristics of the model parameters, the forgetting factor is added to the outer loop(time loop) updates.

$$R_i^t = r \times R_i^{t-1} + (1-r) \times \hat{\epsilon}_{i-1}(t) \hat{\eta}_{i-1}(t-i), i = 1, 2, \dots, k, \dots, K \quad (18)$$

$$\hat{\Gamma}(0)^t = r \times \hat{\Gamma}(0)^{t-1} + (1-r) \times x_t x_t' \quad (19)$$

In Equation 18, R_i^t is the mean of the covariance matrix for $\hat{\epsilon}_{i-1}(t)$ and $\hat{\eta}_{i-1}(t-i)$ in time t . Similarly, Equation 13 can be rewritten as:

$$\hat{\eta}_k(t-k) = \hat{\eta}_{k-1}(t-k) - b_k(k) \hat{\epsilon}_{k-1}(t) \quad (20)$$

So the calculation process of double iteration algorithm is illustrated in Figure 1.

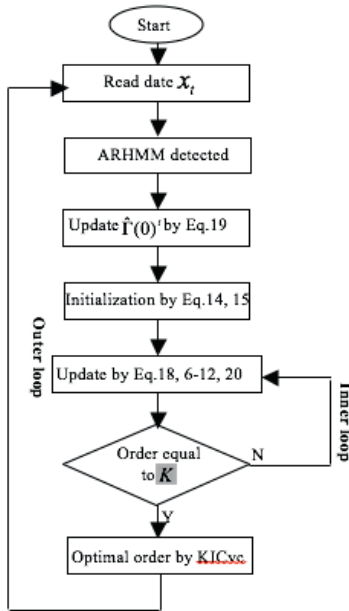


Figure 1. Flow chart of double iteration algorithm

Implementation of Order Self-learning ARHMM Detection Algorithm

The traditional ARHMM structure is composed of two parts (Wang, & Chiang, 2008): one is Markov chain, which is expressed as initial state probability π and state transition matrix $A = (a_{ij})_{N \times N}$, $a_{ij} = P(S_t = s_j | S_{t-1} = s_i)$, $1 \leq i, j \leq N$, in which S_t is the state at time t , N is the total state for HMM, and $P(\cdot)$ is a

conditional probability. The other is expressed as observation probability matrix $B = (b_{ij})_{N \times N}$ calculated by AR model.

$$b_{ij} = P(\hat{x}_t | S_t = s_j) = N(\hat{x}_t | \sum_{i=1}^k a_k(i) x_{t-i}, \hat{\Sigma}_k) \quad (21)$$

In Equation 21, $N(\cdot)$ is Gauss function, and $\hat{\Sigma}_k$ is estimated the variance of Gauss distribution.

ARHMM outlier detection algorithm also composed of two steps:

One step-- Preliminary detection

From Equation 1, we can see that there is a deviation between estimated process data by AR model and real process data.

$$x_t = \hat{x}_t + \epsilon_k(t) \quad (22)$$

If the deviation $\epsilon_k(t)$ is only noise, it obeys Gauss distribution. So the preliminary criteria for outlier detection are to determine the probability that the deviation follows Gauss distribution.

$$P\{x_t | s_t = 1\} = \exp\{-\frac{1}{2} \hat{\epsilon}_p(t)' \hat{U}^{t-1}_p \hat{\epsilon}_p(t)\} \quad (23)$$

In Equation 23, $s_t = 1$ indicates that the real data detected is normal, $s_t = 0$ means it is the outlier. So the detection criteria can be expressed that:

$$\text{if } P\{x_t | s_t = 1\} \geq 0.5, \text{ then } s_t = 1; \quad (24)$$

$$\text{if } P\{x_t | s_t = 1\} < 0.5, \text{ then } s_t = 0;$$

In Equation 23, the subscript p is the optimal model order calculated by KICvc criteria whose expression is:

$$KIVvc(i) = n \ln \left(\text{ave} \hat{\Sigma}_i^t \right) + \frac{nm(2im + m + 1)}{n - im - m - 1} + \frac{nm}{n - im - (m - 1) / 2} + \frac{2m^2 i + m^2 - m}{2n}, \quad i = 1, 2, \dots, K \quad (25)$$

In Equation 25, $\text{ave} \hat{\Sigma}_i^t, i = 1, 2, \dots, K$ is the mean of residual $\epsilon_k(t)$ under various model order (Bilmes, 2006).

$$\text{ave} \hat{\Sigma}_i^t = \frac{\text{sum} \hat{\Sigma}_i^t}{t-1} \quad (26)$$

$$\text{sum} \hat{\Sigma}_i^t = \text{sum} \hat{\Sigma}_i^{t-1} + \hat{\epsilon}_i(t-1) \hat{\epsilon}_i(t-1)' \quad (27)$$

Two step-- Final detection

In final detection, the result of Preliminary detection is the observed value of HMM. So the final detection result obtained by Viterbi algorithm (Abd-Krim, 2006):

$$\begin{aligned} \varphi_0(k) &= \ln \pi_k \cdot b_{0k} \\ \varphi_i(k) &= \max_{i=1, \dots, N} \{\varphi_{i-1}(i) + \ln a_{ik}\} + \ln b_{ik}, k = 1, \dots, N \end{aligned} \quad (28)$$

For improved ARHMM algorithm, when the data at t time is detected, the data before t time already is detected. So the traditional Viterbi algorithm is request into:

$$\begin{aligned} \varphi_t(1) &= a_{i1} \cdot P_t(1); & \varphi_t(0) &= a_{i0} \cdot P_t(0) \\ P_t(1) &= P\{x_t | s_t = 1\} \text{ calculated by Eq. (23)} \\ P_t(0) &= 1 - P_t(1) \end{aligned} \quad (29)$$

$$\begin{aligned} \text{if } \varphi_t(1) > \varphi_t(0) \text{ } x_t \text{ is normal} \\ \text{if } \varphi_t(1) \leq \varphi_t(0) \text{ } x_t \text{ is outlier} \end{aligned} \quad (30)$$

Parameters Updating by Outlier

The parameters of order self-learning ARHMM algorithm need update online, and the parameters are estimated residual mean $\text{ave} \hat{\Sigma}_i^t$, State transition matrix A , $\hat{\epsilon}_\phi(t)$, $\hat{\eta}_\phi(t)$, $\hat{\Gamma}^t(0)$ and in improved BDT algorithm. Specific update algorithm is as follows: